



**HAL**  
open science

## Tomato GDSL1 is required for cutin deposition in the fruit cuticle

Anne-Laure Girard, Fabien F. Mounet, Martine Lemaire-Chamley, Cedric Gaillard, Khalil K. Elmorjani, Julien Vivancos, Jean-Luc Runavot, Bernard Quemener, Johann J. Petit, Veronique Germain, et al.

► **To cite this version:**

Anne-Laure Girard, Fabien F. Mounet, Martine Lemaire-Chamley, Cedric Gaillard, Khalil K. Elmorjani, et al.. Tomato GDSL1 is required for cutin deposition in the fruit cuticle. *The Plant cell*, 2012, 24 (7), pp.3119-3134. 10.1105/tpc.112.101055 . hal-02650850

**HAL Id: hal-02650850**

**<https://hal.inrae.fr/hal-02650850>**

Submitted on 29 May 2020

**HAL** is a multi-disciplinary open access archive for the deposit and dissemination of scientific research documents, whether they are published or not. The documents may come from teaching and research institutions in France or abroad, or from public or private research centers.

L'archive ouverte pluridisciplinaire **HAL**, est destinée au dépôt et à la diffusion de documents scientifiques de niveau recherche, publiés ou non, émanant des établissements d'enseignement et de recherche français ou étrangers, des laboratoires publics ou privés.

## Tomato GDSL1 Is Required for Cutin Deposition in the Fruit Cuticle

Anne-Laure Girard, Fabien Mounet, Martine Lemaire-Chamley, Cédric Gaillard, Khalil Elmorjani, Julien Vivancos, Jean-Luc Runavot, Bernard Quemener, Johann Petit, Véronique Germain, Christophe Rothan, Didier Marion and Bénédicte Bakan

*Plant Cell* 2012;24;3119-3134; originally published online July 17, 2012;

DOI 10.1105/tpc.112.101055

This information is current as of October 2, 2013

<b>Supplemental Data</b>	<a href="http://www.plantcell.org/content/suppl/2012/07/03/tpc.112.101055.DC1.html">http://www.plantcell.org/content/suppl/2012/07/03/tpc.112.101055.DC1.html</a>
<b>References</b>	This article cites 101 articles, 42 of which can be accessed free at: <a href="http://www.plantcell.org/content/24/7/3119.full.html#ref-list-1">http://www.plantcell.org/content/24/7/3119.full.html#ref-list-1</a>
<b>Permissions</b>	<a href="https://www.copyright.com/ccc/openurl.do?sid=pd_hw1532298X&amp;issn=1532298X&amp;WT.mc_id=pd_hw1532298X">https://www.copyright.com/ccc/openurl.do?sid=pd_hw1532298X&amp;issn=1532298X&amp;WT.mc_id=pd_hw1532298X</a>
<b>eTOCs</b>	Sign up for eTOCs at: <a href="http://www.plantcell.org/cgi/alerts/ctmain">http://www.plantcell.org/cgi/alerts/ctmain</a>
<b>CiteTrack Alerts</b>	Sign up for CiteTrack Alerts at: <a href="http://www.plantcell.org/cgi/alerts/ctmain">http://www.plantcell.org/cgi/alerts/ctmain</a>
<b>Subscription Information</b>	Subscription Information for <i>The Plant Cell</i> and <i>Plant Physiology</i> is available at: <a href="http://www.aspb.org/publications/subscriptions.cfm">http://www.aspb.org/publications/subscriptions.cfm</a>

# Tomato GDSL1 Is Required for Cutin Deposition in the Fruit Cuticle <sup>©W</sup>

Anne-Laure Girard,<sup>a,1</sup> Fabien Mounet,<sup>a,1</sup> Martine Lemaire-Chamley,<sup>b,c</sup> Cédric Gaillard,<sup>a</sup> Khalil Elmorjani,<sup>a</sup> Julien Vivancos,<sup>b</sup> Jean-Luc Runavot,<sup>a</sup> Bernard Quemener,<sup>a</sup> Johann Petit,<sup>b,c</sup> Véronique Germain,<sup>b,c</sup> Christophe Rothan,<sup>b,c</sup> Didier Marion,<sup>a</sup> and Bénédicte Bakan<sup>a,2</sup>

<sup>a</sup>Unité Biopolymères, Interactions, Assemblages, Institut National de la Recherche Agronomique, F-44316 Nantes cedex 3, France

<sup>b</sup>Institut National de la Recherche Agronomique, Unité Mixte de Recherche 1332 Biologie du Fruit et Pathologie, F-33140 Villenave d'Ornon, France

<sup>c</sup>Université de Bordeaux, Unité Mixte de Recherche 1332 Biologie du Fruit et Pathologie, F-33140 Villenave d'Ornon, France

**The plant cuticle consists of cutin, a polyester of glycerol, hydroxyl, and epoxy fatty acids, covered and filled by waxes. While the biosynthesis of cutin building blocks is well documented, the mechanisms underlining their extracellular deposition remain unknown. Among the proteins extracted from dewaxed tomato (*Solanum lycopersicum*) peels, we identified GDSL1, a member of the GDSL esterase/acylhydrolase family of plant proteins. GDSL1 is strongly expressed in the epidermis of growing fruit. In GDSL1-silenced tomato lines, we observed a significant reduction in fruit cuticle thickness and a decrease in cutin monomer content proportional to the level of GDSL1 silencing. A significant decrease of wax load was observed only for cuticles of the severely silenced transgenic line. Fourier transform infrared (FTIR) analysis of isolated cutins revealed a reduction in cutin density in silenced lines. Indeed, FTIR-attenuated total reflectance spectroscopy and atomic force microscopy imaging showed that drastic GDSL1 silencing leads to a reduction in ester bond cross-links and to the appearance of nanopores in tomato cutins. Furthermore, immunolabeling experiments attested that GDSL1 is essentially entrapped in the cuticle proper and cuticle layer. These results suggest that GDSL1 is specifically involved in the extracellular deposition of the cutin polyester in the tomato fruit cuticle.**

## INTRODUCTION

Cuticle is a complex assembly of a hydrophobic biopolymer (i.e., cutin, coated and filled with waxes). Waxes are mixtures of aliphatic molecules with very long hydrocarbon chains, including alkanes, fatty alcohols, aldehydes, acids, and esters as well as secondary metabolites (i.e., cyclic triterpenoids, phenylpropanoids, and phenolics) (Waltson, 1990; Schnurr et al., 2004). Cutin, the skeleton of cuticle, is a polyester of  $\omega$ - and midchain hydroxylated C<sub>16</sub> and/or C<sub>18</sub> fatty acids and glycerol. Structural characterizations of plant cuticle have delineated two different regions, the cuticle proper, containing only cutin and waxes, and the cuticle layer, which also includes cell wall polysaccharides (Jeffree, 2006).

Cutin plays a major role as the primary physical barrier in plant cuticles experiencing biotic and abiotic stress (Reina-Pinto and Yephremov, 2009). Cutin could also play a major role in plant morphogenesis. Actually, cutin regulates cell adhesion during plant development by preventing organ fusion as observed in

*Arabidopsis thaliana* cutin-deficient mutants (Sieber et al., 2000; Nawrath, 2006; Shi et al., 2011) or by regulating hull adhesion in cereal grains (Taketa et al., 2008). Taken together, these observations underline the importance of determining cutin structure and biosynthesis to delineate the biological function of plant cuticles.

Considerable progress in the understanding of cutin formation has been gained by the screening of *Arabidopsis* organ fusion mutants (Wellesen et al., 2001; Schnurr et al., 2004; Xiao et al., 2004; Bessire et al., 2007; Kannangara et al., 2007) and the discovery of Wax inducer/Shine 1 (WIN1/SHN1) protein, a transcription factor that regulates wax and cutin biosynthesis (Aharoni et al., 2004; Kannangara et al., 2007; Shi et al., 2011). The formation of the extracellular cutin polymer involves three major steps: (1) synthesis of the cutin precursors, (2) their translocation and diffusion in the apoplast, and (3) their polymerization.

Cutin monomers (i.e., hydroxy- and epoxy-fatty acids) are synthesized in epidermal cells. The major pathway involves  $\omega$ -hydroxylases, such as HOTHREAD oxidase (HTH) or cytochrome P450 of the CYP86A subfamily (Wellesen et al., 2001; Kurdyukov et al., 2006a), long-chain acyl-CoA synthases (Schnurr et al., 2004; Lü et al., 2009), and glycerol-3-phosphate acyltransferases (Beisson et al., 2007; Li et al., 2007b; Yang et al., 2010). Midchain hydroxylation of  $\omega$ -hydroxylpalmitate to form the dihydroxypalmitate is catalyzed by a specific cytochrome P450, CYP77A6 (Li-Beisson et al., 2009). Another pathway, the lipoygenase-peroxygenase pathway, could be involved in the midchain epoxidation of C18 unsaturated fatty acids (Blee and Schuber, 1993). Glycerol-3-phosphate

<sup>1</sup> These authors contributed equally to this work.

<sup>2</sup> Address correspondence to bakan@nantes.inra.fr.

The author responsible for distribution of materials integral to the findings presented in this article in accordance with the policy described in the Instructions for Authors (www.plantcell.org) is: Bénédicte Bakan (bakan@nantes.inra.fr).

<sup>©</sup> Some figures in this article are displayed in color online but in black and white in the print edition.

<sup>W</sup> Online version contains Web-only data.

www.plantcell.org/cgi/doi/10.1105/tpc.112.101055

acyltransferases catalyze the transfer of acyl-CoAs to glycerol-3-phosphate to form lysophosphatidic acid, a precursor of acylglycerols and especially of monoacylglycerol (Pollard et al., 2008), an elemental building block of the cutin polymer (Graça et al., 2002). In *Arabidopsis*, GLYCEROL-3-PHOSPHATE ACYLTRANSFERASE4 (GPAT4) and GPAT6 are involved in cutin biosynthesis and are unique glycerol-3-phosphate acyltransferases containing a regio-selective acyltransferase and a phosphatase leading to the production of 2-monoglycerides (Yang et al., 2010). The apoplastic secretion of sn-2 monoglycerides observed upon the ectopic overexpression of the suberin-associated and sn-2 regioselective GPAT5 strengthened their role as synthons (i.e., biosynthetic monomers) for extracellular cutin polymerization (Li et al., 2007a; Yang et al., 2010). Finally, a cytosolic acyltransferase of the BAHD family of acyltransferase with in vitro diacylglycerol-acyltransferase activity was involved in the incorporation of dihydroxypalmitate into the cutin of *Arabidopsis* flowers. It was suggested that this diacylglycerol-acyltransferase could be involved in the formation of other cutin precursors, cutin oligomers, or triacylglycerols (Rani et al., 2010; Panikashvili et al., 2011), whereas members of the BAHD family of acyltransferase usually catalyze the acylation of secondary metabolites (D'Auria, 2006).

The transport of hydrophobic cutin precursors and their polymerization in the aqueous cell wall-filled apoplast are less documented. ATP binding cassette (ABC) transporters located in the plasmalemma of epidermal cells are required for both cutin and wax deposition (Bessire et al., 2007; Panikashvili et al., 2007, 2011; Bird, 2008; Chen et al., 2011) and could be involved in the apoplastic translocation of the cutin precursors. Owing to their extracellular localization, generally close to cuticle surfaces, and their ability to bind lipids in a hydrophobic cavity, lipid transfer proteins often have been proposed to fulfill this function (Douliez et al., 2000; Blein et al., 2002). However, no functional genomics study has confirmed this transport function or the involvement of these proteins in cuticle assembly.

Although the polyesterification of cutin monomers through a chemical process could not be excluded (Heredia-Guerrero et al., 2009), most studies since the pioneering work of Croteau and Kolattukudy (1973, 1974) have focused on an enzyme-catalyzed mechanism of polymerization. The  $\alpha/\beta$  hydrolase BODYGUARD (BDG) has been identified as a candidate protein to fulfill this role in *Arabidopsis*. However, this protein does not fit perfectly with its proposed function in cutin polymerization because mutation of this protein induces other pleiotropic effects besides cuticle modification (Kurdyukov et al., 2006b).

Recently, the proteins of the Gly-Asp-Ser-Leu family of esterases/acylhydrolases, commonly called GDSL-lipases, which, like BDG, belong to the  $\alpha/\beta$  hydrolase family, have triggered considerable interest. Indeed, GDSL-lipases are expressed in epidermal cells of the peel, close to the cuticular membranes (Lemaire-Chamley et al., 2005; Reina et al., 2007; Mintz-Oron et al., 2008; Matas et al., 2010; Yeats et al., 2010), and the expression of an *Arabidopsis* GDSL-lipase is upregulated by WIN1/SHN1, a transcription factor that regulates cutin deposition (Kannangara et al., 2007; Shi et al., 2011). In addition, GDSL-lipases are synthesized as preproteins containing signal peptides predicted to facilitate extracellular exportation. This

extracellular location was confirmed for most characterized GDSL-lipases in latex (Abdelkafi et al., 2009), in nectar (Kram et al., 2008), in the secretome of plant cells (Oh et al., 2005; Naranjo et al., 2006; Hong et al., 2008; Kusumawati et al., 2008), and in sporollenin, a cutin-like polymer of the pollen coat (Updegraff et al., 2009). However, to date, most of the studies have highlighted the role of GDSL-lipases in the tolerance of plants to biotic and abiotic stress (Oh et al., 2005; Naranjo et al., 2006; Hong et al., 2008). Nevertheless, through the cuticular defects induced by the ectopic overexpression of an *Arabidopsis* pollen GDSL-lipase (CUTICLE DESTRUCTING FACTOR1 [CDEF1]), Takahashi et al. (2010) recently suggested that CDEF1 could be a plant cutinase.

Tomato (*Solanum lycopersicum*) has recently become an attractive plant model because of the development of functional genomic tools and the recent completion of the tomato genome sequence. In addition, the cuticle of tomato fruits can be isolated (López-Casado et al., 2007), and its cutin polymer was found to be dominated by a single monomer (i.e., 9,16 hydroxy-palmitic acid) (Graça et al., 2002). Furthermore, the tomato fruit is as-tomatous, providing a cuticle with an intact surface. In this study, we characterize tomato GDSL1, the main GDSL-lipase protein expressed in the epidermis of developing tomato fruit. Silencing of *GDSL1* expression by the RNA interference (RNAi) strategy alters cutin load and cutin structure of the fruit. GDSL1 localized to both the cuticle proper and cuticle layer. We therefore conclude that the extracellular and cutin-embedded GDSL-lipase is specifically required for the formation of the cutin polymer.

## RESULTS

### Proteome Analysis of Tomato Fruit Cutinized Exocarp Highlights an Epidermis GDSL-Lipase

One of the most abundant proteins identified from tomato cutin, with 54% sequence coverage, was a GDSL-lipase (accession number SGN-U585129) (Figure 1A). Although GDSL-lipases form a multigenic family in tomato, this protein, hereafter named GDSL1, was the sole GDSL-lipase identified. A proteome analysis performed on material released from tomato fruits immersed in methanol/chloroform identified two additional GDSL-lipases (SGN-U583101 and SGN-U579520) and a peptide of GDSL1 (Yeats et al., 2010). A large number of cell wall-modifying proteins or cellular proteins were also identified. Real-time RT-PCR analysis of *GDSL1* expression in tomato fruit tissues indicated that *GDSL1* transcripts accumulate specifically in the exocarp (Figure 1B). The highest transcript accumulation was reached at 20 d postanthesis (DPA) in the 'Aïsa Craig' tomato fruit (see Supplemental Figure 1 online) (i.e., during the cell expansion phase) (Mounet et al., 2009).

The full-length *GDSL1* cDNA sequence (1042 bp) revealed an open reading frame specifying a 362-amino acid putative protein with a predicted N-terminal signal peptide of 19 residues (see Supplemental Figure 2 online). Like 99 of the 107 *Arabidopsis* GDSL-lipases (Ling, 2008), tomato GDSL1 is predicted to be located extracellularly. Although the overall sequence of the members of this large multigenic family is barely conserved, five sequence blocks are highly conserved and were also found in

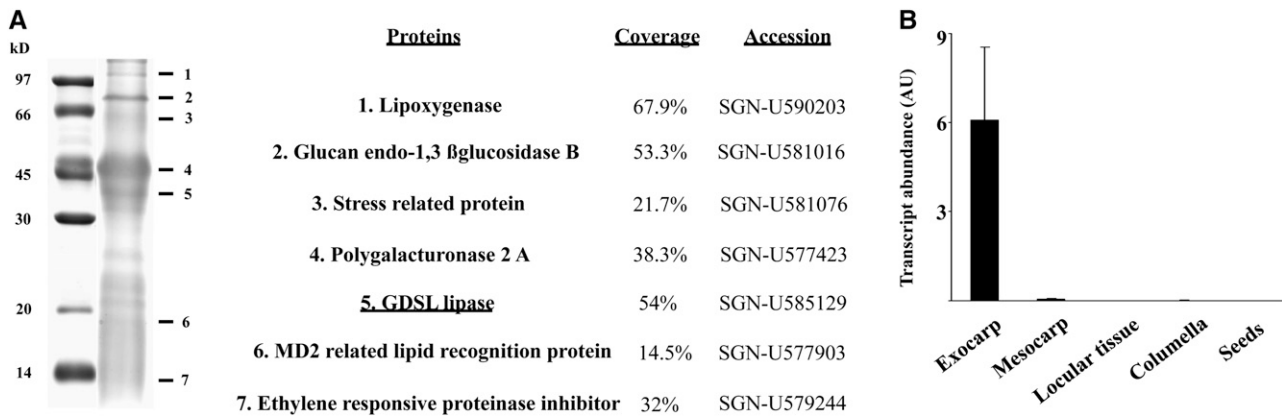


**Figure 1.** Isolation and Characterization of a GDSL-Lipase from Tomato Cutinized Exocarp.

(A) SDS-PAGE of proteins extracted from red ripe tomato fruits. Liquid chromatography coupled to tandem mass spectrometry analysis of trypsin-digested peptide fragments allowed the identification of the most abundant proteins. Column 2 refers to amino acids sequence coverage and column 3 to accession numbers in the SGN database (<http://solgenomics.net/index.pl>).

(B) Transcript abundance of GDSL1 measured by real-time RT-PCR in exocarp, mesocarp, locular tissue, columella, and seeds at 20 DPA. AU, arbitrary units. Vertical bars represent *sd* ( $n = 4$ ).

tomato GDSL1 (see Supplemental Figure 2 online). The three amino acids of the catalytic triad are present in block I (Ser-32) and block V (His-326), whereas, as previously suggested, the Asp residue is either localized to block III (Asp-166) (Upton and Buckley, 1995) or block V (Asp-323), immediately upstream of His (Akoh et al., 2004).

### The P35S-SIGDSL1 RNAi Transgenic Lines Display Major Changes in Fruit Cuticle

To delineate the function of *GDSL1* in tomato, we generated *GDSL1* RNAi-silenced tomato transgenic lines (P35S-SIGDSL1 RNAi lines), hereafter named L-10, L-4, L-3, and L-17, which showed moderate to severe downregulation of *GDSL1*. *GDSL1* transcript levels were highest in 12-DPA fruit and decreased thereafter during fruit development. At 12 DPA, silencing appeared less effective in L-10 and L-4, whereas L-3 and L-17 presented an ~70 to 95% reduction in *GDSL1* transcript abundance (Figure 2A). From 20 DPA on, all of the transgenic lines showed a reduction in the expression of *GDSL1*, ranging from 78% (L-4) to 98% (L-17) compared with the wild type. Immunoblotting revealed a decrease in GDSL1 content in all transgenic lines, especially in line L-17, in which protein could not be detected at any stage of development (Figure 2B).

Homozygous transgenic plants were grown in the greenhouse over several years at different seasons. Despite the various environmental conditions, no effect on vegetative or reproductive organ development was revealed, except for the appearance of glossy fruits with increased brightness in the two transgenic lines with the greatest degree of silencing (i.e., L-3 and L-17) (Figure 3A). Fruit surface, extrapolated from fruit diameter measurements, appeared unchanged (Figure 3A), indicating that fruit brightness increase was not related to fruit size per se.

Unlike the previously described *cwp1* tomato mutants (Hovav et al., 2007), no symptom of dehydration was observed in any of the mutant fruits under greenhouse conditions. In postharvest

accelerated dehydration conditions, a significant difference in water loss was observed only for L-3 and L-17 fruits (Figure 3B). Therefore, the decrease in *GDSL1* transcripts did not induce severe modifications in water permeability of fruit cuticles, except for the severely affected lines, L-3 and L-17. To test this hypothesis, we further checked the cuticle permeability to toluidine blue (TB), a hydrophilic dye of phenothiazinium salt, in 20-DPA fruits. An increase in TB uptake was observed in fruits from the transgenic lines L-4, L-3, and L-17, suggesting structural defects in the fruit cuticle (Figure 3C). The TB staining was patchily distributed, forming dots or clusters of dots. No fruits displayed an epidermal surface with continuous staining as observed for fruits of the *cwp1* tomato mutants (Hovav et al., 2007). Overall, these results support the notion that the fruit cuticle of the RNAi lines is somewhat disrupted, but that, even in the most severely affected transgenic line (L-17), is partially preserved.

Examination of cuticle thickness using Sudan Red (Figures 4A to 4C) revealed a gradual decrease in cuticle thickness from the wild type to L-17 fruit (wild type  $\geq$  L-10 > L-4 > L-3 > L-17), in full agreement with the concomitant decrease in cuticle load per fruit surface unit (Figure 4D). As previously described (Buda et al., 2009; Isaacson et al., 2009), fruit cuticle spreads within the first layers of epidermis cells, resulting in encased cutinized epidermal cells in the wild-type fruit (Figure 4A). Measurements of cuticle thickness were therefore taken at two points: (1) at the junction of two epidermal pavement cells, from the external cuticular layer to the subepidermal cuticular material (Figure 4B), and (2) on top of epidermis cells, where the cuticle layer is thinner (Figure 4C). In fruits from L-10 and L-4, the cuticular layer surrounded all the fruit pavement epidermal cells as in wild-type fruit. By contrast, cuticularization of anticlinal walls and subepidermal deposition of cuticular material was significantly reduced in L-3 and almost disappeared in L-17 (Figure 4A). The most striking change in transgenic lines was the impressive reduction in cuticle thickness above the pavement epidermal

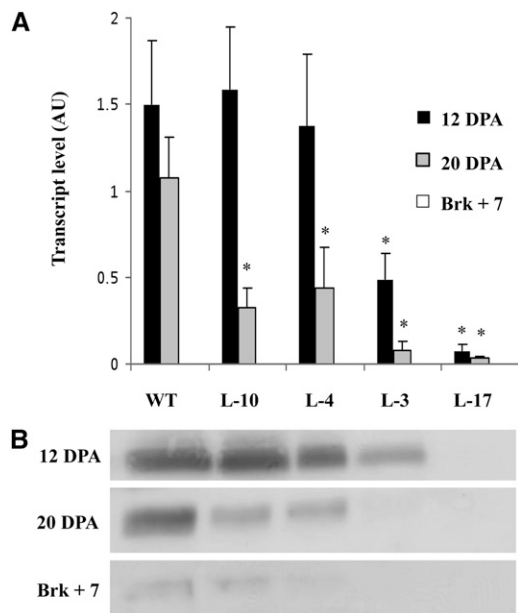


**Figure 2.** Downregulation of *GDSL1* Expression and Protein Level in Fruits of P35S-SIGDSL1 RNAi Plants.

Analyses were performed at three stages of fruit development: 12 DPA, 20 DPA, and breaker + 7 d (Brk+7) in wild-type (WT) and transgenic lines (L-10, L-4, L-3, and L-17).

**(A)** *GDSL1* expression level measured by real-time RT-PCR. Histograms represent mean transcript levels (AU, arbitrary units) of four biological replicates, and vertical bars represent sd. *GDSL1* expression was very low at breaker + 7 stage. Asterisks indicate a significant difference with fruits of the wild type (*t* test,  $P < 0.05$ ).

**(B)** *GDSL1* level in fruits of 12-DPA, 20-DPA, and breaker + 7 stages analyzed by immunoblots.

cells, especially in L-3 and L-17, where cuticle was reduced to a thin film at the surface of the fruit (Figure 4C). Because mutation in the epidermal-expressed gene *BDG*, proposed to control cuticle formation, also affects epidermis proliferation/differentiation status in *Arabidopsis* (Kurdyukov et al., 2006b), we examined the collenchyma cell layers underneath the epidermis. However, no visible alteration of epidermal cells was observed in fruit of the RNAi lines, even in L-17 (Figure 4E). Altogether, these results suggest that silencing of *GDSL1*, which induces major changes in the cuticle, has no other apparent pleiotropic effect on plant and fruit development.

### ***GDSL1* Is Embedded in the Cutinized Matrix of Tomato Cuticle**

To gain insight into the relationship between *GDSL1* and cuticle biosynthesis, the localization of *GDSL1* in the cuticle was monitored (Figure 5; see Supplemental Figure 3 online). According to the expression profile of *GDSL1* (Figure 2), immunolocalization of the corresponding protein was performed in the exocarp of wild-type and L-17 and L-3 plants harvested at 20 DPA. In wild-type fruits, the cuticle forms an electron dense layer of  $\sim 6 \mu\text{m}$  (see Supplemental Figure 3D online) deposited

over a less dense layer corresponding to cell walls. Cell wall cutinization of wild-type fruits occurs between epidermal cells, thus forming anticlinal pegs (Figure 4). In the L-17 line, anticlinal pegs are almost absent and the cuticular layer is very thin but nevertheless regularly deposited ( $\sim 1.5 \mu\text{m}$ ) on the surface of the epidermal cells (Figures 4A and 5C to 5I).

Both immunogold and fluorescence labeling revealed that *GDSL1* was located in the cuticular layer and to a lesser extent in the cytoplasm of the underlying epidermal cells (Figure 5). Intense labeling was observed in the anticlinal pegs and in the cutin region between epidermal cells, which begin to undergo cutinization at this stage of fruit development (Figure 5J). Auramine staining of 20-DPA fruits allowed the distinction between the cuticle proper and cuticle layer (see Supplemental Figure 3 online). *GDSL1* labeling was observed in the both cuticle layer and cuticle proper, thus confirming that this protein is associated to cutin. Finally, no labeling was observed in the noncutinized cell wall layer of the exocarp (see Supplemental Figure 3 online).

In agreement with *GDSL1* expression, the level of detected protein was greater in the wild type and in L-3 than in L-17 in both experimental conditions (Figure 5).

### ***GDSL1* Silencing Specifically Impacts Cutin Monomer Deposition**

The effect of *GDSL1* silencing on cutin and wax biosynthesis was further characterized in red ripe fruits (Table 1). Consistent with the reduction in cuticle thickness (Figure 4), the level of cutin monomers per surface unit decreased proportionally to the reduction in *GDSL1* expression (Table 1). Indeed, the total amount of cutin monomers represented 95.2% (L-10), 52% (L-4), 30% (L-3), and only 5% (L-17) of the level in wild-type fruits. In all lines, dihydroxyhexadecanoic acid was the most abundant monomer. The relative proportion of the different cutin constituents was generally well conserved within the various transgenic lines, except for 16-hydroxyhexadecanoic acid, which gradually decreased from 3% in the wild type (and L-10) to 0.7% in L-17, while the hexadecanoic acid increased from 0.5% (the wild type) to 2.4% (L-17).

We further investigated the effect of *GDSL1* silencing on wax deposition in fruit. About half of the total waxes quantified were alkanes, 24% were fatty acids, and 23% were plant triterpenoids and sterols. Waxes were mostly composed of C31 alkanes (26% of total) and  $\delta$ ,  $\beta$ , or  $\alpha$  amyriols (19.5%), in agreement with previous reports (Leide et al., 2007; Saladié et al., 2007; Isaacson et al., 2009). No significant difference in wax content and composition were detected when transgenic lines L-10, L-4, and L-3 are compared with the wild type (Table 1). Wax load was significantly affected only in the most severely affected L-17 line where the wax content dropped 10-fold when compared with the wild type and displayed a significant reduction in the proportion of sterol and terpenoid compounds. Thus, the decrease in wax content per surface unit did not follow the decrease in the corresponding cutin monomer content.

No accumulation of cutin monomers or monoglycerides (i.e., the building blocks of cutin) (Pollard et al., 2008) was detected in the fruit wax fractions or in the exocarp lipid extracts of the RNAi

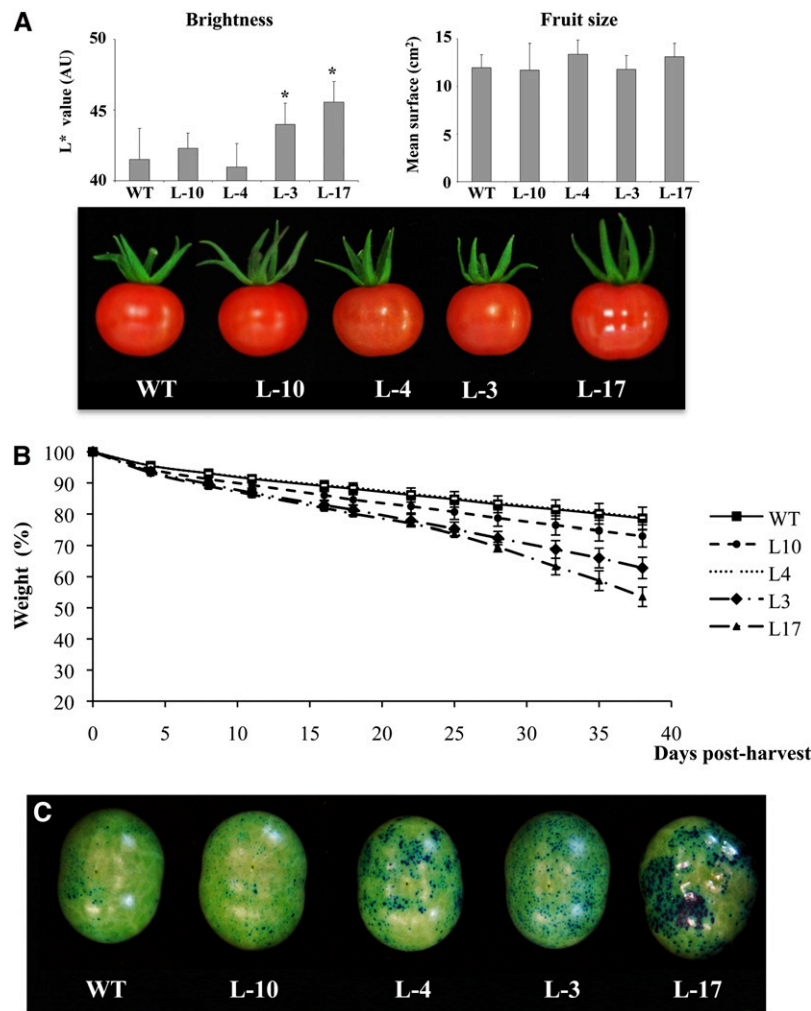


**Figure 3.** Analysis of Fruit Brightness, Fruit Size, Postharvest Water Loss, and Permeability in P35S-SIGDSL1 RNAi Plants Compared with the Wild Type.

**(A)** Fruit brightness was measured using an L\*a\*b\* colorimeter, where L corresponds to luminance in red ripe fruits at breaker + 7. Fruit size was represented using mean fruit surface value (extrapolated from diameter measurements). Comparisons were made between wild-type and transgenic lines (L-10, L-4, L-3, and L-17). Vertical bars represent  $sd$  ( $n = 13$  to 19). Asterisks indicate a significant difference with fruits of the wild type ( $t$  test,  $P < 0.05$ ). AU, arbitrary units; WT, the wild type.

**(B)** Postharvest water loss of red ripe fruits from wild-type plants and L10, L-4, L-3, and L-17 transgenic lines was measured over a 38-d period. Values are means ( $\pm sd$ ) of six samples from three biological replicates stored at 30°C.

**(C)** TB (1% [v/v] solution) coloration of 20-DPA fruits from wild-type and transgenic lines.

[See online article for color version of this figure.]

lines. Accordingly, no significant alteration in osmium-stained lipids was detected by transmission electron microscopy (TEM) in 20-DPA exocarps from L-17 compared with the wild type (see Supplemental Figure 4 online). In particular, we do not detect any increase in plastoglobules, as observed in cuticular *Arabidopsis ltpg1* mutants (Lee et al., 2009b), or the presence of lipid inclusions, as reported for ABC transporter *Arabidopsis* mutants impaired in the transport of cutin precursors (Bird et al., 2007; Bessire et al., 2011).

Finally, we analyzed the expression of some tomato candidate genes known to be involved in the *Arabidopsis* cutin

biosynthesis pathway. Real-time RT-PCR analysis was performed in the exocarp of 20-DPA fruits from the most severely altered lines L-3 and L-17. The results were compared with those of the wild type and with the mildly affected L-10 line, which displays a fruit cutin composition roughly similar to that of wild-type plants (see Supplemental Figure 5 and Supplemental Table 1 online). A significant downregulation of *CYP86A7*, *GPAT4*, and *GPAT6* and of three *HTH*-like genes as well as one lipid transfer protein gene (*LTPG2*) was observed in L-3 and L-17, in which *GDSL1* is strongly silenced. These results suggest a possible feedback regulation of the cutin biosynthesis

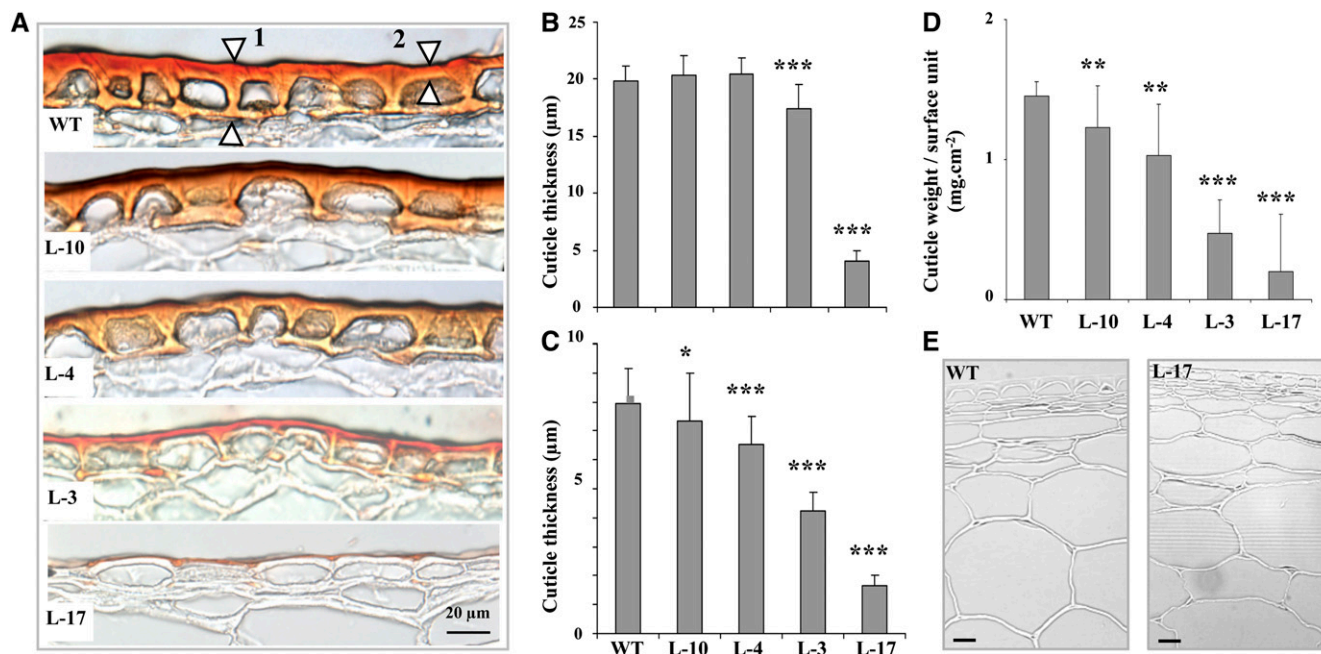


**Figure 4.** Cuticle Thickness in Fruits of Wild-Type and P35S-SIGDSL1 RNAi Plants.

**(A)** Cross section of fruit exocarp from wild-type and transgenic lines L-10, L-4, L-3, and L-17 (light microscopy). Sudan Red staining revealed cuticle and cutinized cells of the first exocarp cell layer. WT, the wild type.

**(B)** and **(C)** Cuticle thickness measurements ( $n = 60$ ) were performed either in the thicker zone at the junction of two pavement cells (arrowhead 1 in **[A]**) **(B)** or in the thinner zone, above a pavement cell (arrowhead 2 in **[A]**) **(C)**.

**(D)** Measurement of cuticle weight per surface unit ( $n = 12$  to 19) in fruits of wild-type and transgenic lines. Vertical bars represent sd. \*, \*\*, and \*\*\* indicate a significant difference with wild-type samples ( $t$  test,  $P < 0.05$ ,  $P < 0.005$ , and  $P < 0.001$ , respectively).

**(E)** Transverse section of 20-DPA fruit exocarp from the wild type and L-17. Bars = 30  $\mu\text{m}$ .

[See online article for color version of this figure.]

pathway, in agreement with the absence of cutin monomer accumulation and the absence of alteration in epidermal cell ultrastructure in the *SIGDSL1*-silenced plants.

#### **GDSL1 Silencing Affects the Structure of the Cutin Polyester**

Attenuated total reflectance (ATR)-Fourier transform infrared (FTIR) analysis was performed on cutin isolated from red ripe fruits (breaker + 7 d). The spectra of dewaxed cutinized fragments are dominated by aliphatic methylene ( $\text{CH}_2$ ) asymmetric and symmetric stretching vibrations of its aliphatic monomers at 2919 and 2850  $\text{cm}^{-1}$  and the carbonyl (CO) stretching vibration of ester bonds at 1729  $\text{cm}^{-1}$  (see Supplemental Figure 6A online). These bands are specific to cutin polyester, since  $\text{CH}_2$  and CO vibrations were either weak or absent, respectively, in the polysaccharide residues obtained after cutin depolymerization (see Supplemental Figure 6B online). When focusing on these stretching vibrations and compared with the wild type, a gradual decrease of absorbance of both  $\text{CH}_2$  and CO bands in transformant lines consistent with the severity of *GDSL1* silencing was observed (Figure 6C). The penetration depth in our experimental conditions (i.e., incident light angle of 45° and a diamond refractive index of 2.4) was estimated to be 0.7  $\mu\text{m}$  at 3000  $\text{cm}^{-1}$  and 1.1  $\mu\text{m}$  at 1000  $\text{cm}^{-1}$  for a refractive index of cutin estimated at 1.5 (da Luz, 2006). Considering the thickness

measurements (Figure 4), this means that, in wild-type and all transformant lines, the infrared signal of methylene and carbonyl groups, which is specific to the cutin polyester, arose mainly from the cutin deposited on the cutinized surface of epidermal cells (from 8 to 1.5  $\mu\text{m}$  for the wild type and L-17, respectively; Figure 4). Therefore, the gradual decrease in absorbance is not mainly related to the decrease in cutin thickness but to the decrease in cutin density. After normalization of the FTIR spectra, no significant differences were observed for methylene bands, indicating that the conformation of aliphatic chains was not significantly affected by *GDSL1* silencing (Figure 6A). Conversely, significant modification in the carbonyl vibration, which is associated with a reduction in *GDSL1* expression, was observed (Figure 6B). The carbonyl stretching vibration centered at 1729  $\text{cm}^{-1}$  displayed a shoulder at 1712  $\text{cm}^{-1}$ . Similar lower frequency carbonyl bands have been observed in the gel state of phospholipids with iso- and anteiso-branched fatty acids (Mantsch et al., 1987) and in polyurethane polymers (Queiroz et al., 2003). Such splitting of the carbonyl band in two components is a common feature, attributed to hydrogen bonding (Blume et al., 1998; Queiroz et al., 2003). The relative increase in the intensity of the 1712  $\text{cm}^{-1}$  shoulder suggests that the ester carbonyl groups are more involved in hydrogen bonding following the decrease in *GDSL1* expression. This could either originate from a higher interaction with the OH groups of the cell

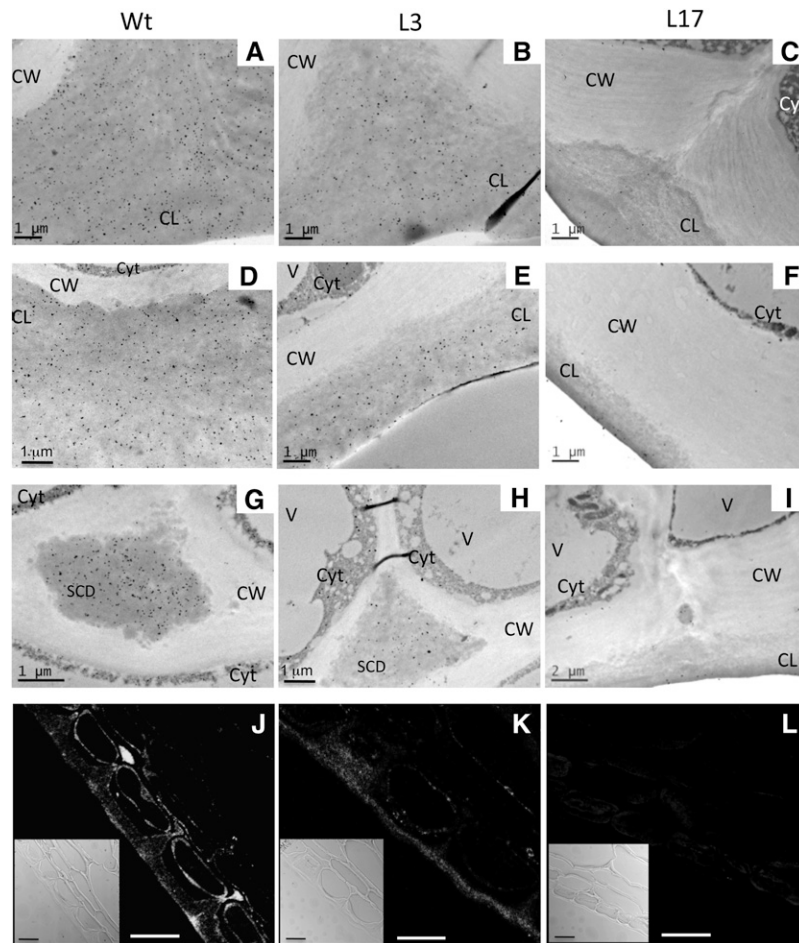


**Figure 5.** Immunolocalization of GDSL1 in the Exocarp of 20-DPA Tomato Fruits from Wild-Type and Transgenic Lines L-3 and L-17.

Tomato exocarp from wild-type ([A], [D], [G], and [J]) and L-3 ([B], [E], [H], and [K]) and L-17 ([C], [F], [I], and [L]) transgenic lines were embedded in LR white resin and labeled with polyclonal anti-GDSL1 antibodies coupled either with gold-conjugated antibodies ([A] to [I]) or fluorescent dyes ([J] to [L], bright field in inset). Black dots represent gold labeling. CL, cuticular layer; CW, cell wall; Cyt, cytoplasm, SCD, subepidermal cutin deposition; V, vacuole; Wt, the wild type. For immunofluorescence labeling ([J] to [L]), bars = 20  $\mu\text{m}$  and the corresponding light micrographs are presented in the inset.

wall polysaccharides or from a modification in the extent of cutin polymerization due to an increase in nonesterified hydroxyl groups in the cutin polymer. By integrating methylene stretching and carbonyl bands specific to the alkyl chain and ester groups of cutin, respectively, it was possible to determine a ratio that can be considered as an index of the extent of polymerization (Figure 6C). When compared with wild-type cutin, a significant decrease in polymerization was observed in L-17, in which *GDSL1* is efficiently silenced.

Since tomato cutin is mainly composed of dihydroxyhexadecanoic acid, it contains more hydroxyl groups than carbonyl groups. Consequently, a lower polymerization index does not necessarily induce a corresponding increase in the carboxylate band. Indeed, the carboxylate vibration at  $1590\text{ cm}^{-1}$  was not observed in both wild-type and L-17 cutin. Besides, it was recently demonstrated that the structure of wild-type tomato cutin is characterized by a high rate of branched linkage, where the

midchain hydroxyl groups are more involved in ester bonds than the omega-hydroxyl groups (Graça and Lamosa, 2010). Therefore, the polymerization defect in L-17 could mainly affect midchain branching of the cutin polymer.

At both 20-DPA and the red ripe stages, atomic force microscopy (AFM) highlighted differences in cutin surface morphology between wild-type and RNAi lines, in particular in L-3 and L-17 (Figure 7; see Supplemental Figure 7 online). For the 20-DPA and red ripe fruits, AFM images showed a continuous cutin displaying the imprint of the underlying epidermal cells. In addition, the comparison of cutin AFM images from 20-DPA and red ripe stages shows that, during fruit development, a higher deposition of cutin occurs in the intercellular region than on the surface of epidermal cells. This result is in good agreement with the intense GDSL1 immunolabeling observed in the cutin region between epidermal cells in 20-DPA wild-type exocarp (Figure 5J).

**Table 1.** Cutin Monomers and Wax Quantification in Isolated Cuticle from Fruits of Wild-Type and Transgenic Lines

Compounds	Wild Type		L-10		L-4		L-3		L-17						
	Mean	sd	%	Mean	sd	%	Mean	sd	%	Mean	sd	%			
Cutin monomers															
Cinnamic acid	5.51	± 6	0.6	4.6	± 0.5	0.6	3.7	± 1.5	0.9	1.1	± 0.6	0.4	0.1	± 0.1	0.3
Palmitic acid	4.8	± 2.4	0.5	5.5	± 2.9	0.7	3.1	± 0.3	0.7	2.4	± 0.9	1.0	1.1	± 0.7	2.4
C18:0 fatty acid	1.6	± 1.0	0.2	1.6	± 1.1	0.2	0.7	± 0.2	0.2	0.6	± 0.2	0.2	0.4	± 0.2	0.9
Hexadecandioic acid	4.7	± 1.5	0.5	3.6	± 0.7	0.4	3.7	± 1.0	0.8	1.3	± 0.6	0.5	0.4	± 0.2	0.9
16-Hydroxyhexadecanoic acid	28.9	± 5.1	3.3	20.2	± 4.0	2.4	14.9	± 2.0	3.4	4.9	± 2.1	<b>1.8</b>	0.3	± 0.1	<b>0.7</b>
16-OH hexadecandioic acid	46.1	± 2.9	5.4	40.1	± 8.9	4.8	23.4	± 6.8	5.1	12.8	± 5.5	4.8	1.3	± 0.2	3.1
9(10),16-diOH hexadecanoic acid	635.6	± 140.3	72.2	631.7	± 193.0	75.1	328.2	± 100.4	71.4	192.3	± 76.7	72.6	31.6	± 4.8	73.1
18-OH octadecanoic acid	64.1	± 6.7	7.4	60.9	± 12.9	7.4	36.4	± 11.5	7.9	20.8	± 9.4	7.7	1.3	± 0.3	3.0
9(10),18-diOH octadecanoic acid	7.2	± 3.8	0.8	8.6	± 4.2	1.0	5.7	± 2.9	1.4	3.2	± 1.1	1.3	0.4	± 0.1	1.0
18-OH-epoxy octadecanoic acid	7.0	± 3.9	0.8	2.7	± 1.0	0.3	1.7	± 0.3	0.4	1.8	± 0.9	0.7	1.2	± 0.4	2.6
Unidentified compounds	73.5	± 23.5	8.2	57.9	± 11.0	7.0	35.9	± 11.6	7.8	22.6	± 5.9	9.0	4.0	± 0.4	9.5
Total ( $\mu\text{g}\cdot\text{cm}^{-2}$ of cuticle)	879.1	± 184.5		837.4	± 232.4		<b>457.4</b>	± <b>126.9</b>		<b>263.7</b>	± <b>91.9</b>		<b>43.3</b>	± <b>7.2</b>	
Wax compounds															
Fatty acids															
C15	1.3	± 0.5	0.4	0.8	± 0.1	0.3	0.8	± 0.1	0.2	0.7	± 0.3	0.3	0.2	± 0.2	0.5
C16	28	± 1.1	8.6	39.9	± 8.6	12.3	<b>42.5</b>	± 4.2	11.7	22.7	± 12.9	9.0	<b>3</b>	± 1.9	7.6
C17	4.5	± 2.8	1.4	1.9	± 0.3	0.6	11.6	± 12.1	3.3	1.5	± 0.9	0.6	0.2	± 0.1	0.5
C18:2	1.6	± 0.5	0.5	1.3	± 0.2	0.4	4.3	± 1.9	1.2	1.2	± 0.6	0.5	0.2	± 0.1	0.4
C18:1	32.8	± 11.0	10.1	24.4	± 7.4	6.7	41.6	± 12.1	11.4	17.6	± 9.4	7.0	<b>0.8</b>	± 0.6	1.9
C18:0	8.1	± 1.7	2.5	8.3	± 1	2.6	7.7	± 3.3	2.1	5	± 2.5	2.0	<b>0.5</b>	± 0.3	1.3
C20	1	± 0.3	0.3	1.1	± 0.5	0.3	0.8	± 0.6	0.2	0.8	± 0.4	0.4	<b>0.02</b>	± 0.0	<b>0.0</b>
Alkanes															
C28	1	± 0.3	0.3	1.4	± 0.2	0.4	1.4	± 0.1	0.4	1	± 0.2	0.5	<b>0.3</b>	± 0.1	<b>0.7</b>
C29	21.1	± 4.1	6.5	28.1	± 2.2	<b>8.7</b>	26.5	± 2.3	7.3	16.7	± 4.2	7.8	<b>3.3</b>	± 0.5	<b>8.8</b>
C30	14.6	± 2.6	4.5	15.2	± 2	4.7	14.6	± 1.4	4	<b>7.6</b>	± 2.3	3.5	<b>1.5</b>	± 0.3	4.0
C31	85.3	± 11.3	26.3	93.7	± 6.1	29.1	89	± 3.8	24.5	68.1	± 14.7	32.4	<b>15.3</b>	± 3.3	40.9
C32	13.3	± 1.3	4.1	14.3	± 2.1	4.4	12.6	± 0.5	3.5	7.7	± 2.4	3.5	<b>1.4</b>	± 0.3	3.7
C33	13.2	± 1.8	4.1	14.8	± 1.9	4.7	15.1	± 2.3	4.2	16.8	± 3.6	<b>8.0</b>	<b>3.4</b>	± 0.8	<b>8.9</b>
Iso-alkanes															
C31	8.4	± 0.8	2.6	8.9	± 0.9	2.8	9.7	± 0.1	2.7	7	± 1.6	3.3	<b>1.6</b>	± 0.3	<b>4.2</b>
C32	1.7	± 0.0	0.5	1.7	± 0.2	0.5	1.8	± 0.1	0.5	1.2	± 0.4	0.5	<b>0.2</b>	± 0.1	0.4
Alcohol															
C16	6.5	± 6.9	2.0	0.5	± 0.2	0.2	0.9	± 0.2	0.2	0.5	± 0.1	0.2	0.1	± 0.1	0.2
C18	2.1	± 0.4	0.7	1.6	± 0.3	0.5	2.4	± 0.5	0.7	1.6	± 0.2	0.8	<b>0.4</b>	± 0.5	0.9
C20	nd	± –	–	1.6	± 0.9	0.5	nd	± –	–	1.4	± 0.8	0.6	0.02	± 0.0	0.0
C29	0.7	± 0.2	0.2	1.2	± 1.3	0.3	0.7	± 0.2	0.2	<b>0.1</b>	± 0.1	<b>0.0</b>	<b>0.1</b>	± 0.2	0.4
Sterols and terpenoids															
Cholesterol	1.6	± 1.1	0.5	0.2	± 0.2	0.0	0.8	± 0.1	0.2	1.1	± 0.3	0.5	0.5	± 0.2	1.3
Stigmasterol	3.1	± 0.5	1.0	1.7	± 1.4	0.5	2.9	± 0.6	0.8	5.1	± 2.3	<b>2.2</b>	<b>0.7</b>	± 0.5	<b>1.7</b>
$\delta$ -Amyrine	24.7	± 1.0	7.6	<b>17.6</b>	± 2.6	<b>5.4</b>	20.8	± 3.5	5.7	10.6	± 5.5	<b>4.6</b>	<b>1.1</b>	± 0.0	<b>3.1</b>
$\beta$ -Amyrine	24.6	± 0.4	7.6	20.7	± 1.9	6.4	25.2	± 3.5	6.9	15.3	± 6.6	6.8	<b>1.5</b>	± 0.3	<b>4.0</b>
$\alpha$ -Amyrine	13.8	± 0.2	4.3	<b>9.8</b>	± 1.1	<b>3.0</b>	11.9	± 1.9	<b>3.2</b>	nd	± –	–	<b>0.6</b>	± 0.0	<b>1.5</b>
Multiflorenol	2.4	± 0.3	0.7	<b>1.7</b>	± 0.2	0.5	2.1	± 0.2	0.6	1.1	± 0.5	0.5	<b>0.02</b>	± 0.0	<b>0.0</b>
$\psi$ -Taraxasterol	1.4	± 0.1	0.4	1.0	± 0.3	0.3	1.5	± 0.5	0.4	1	± 0.6	0.4	<b>0.01</b>	± 0.0	<b>0.0</b>
Taraxasterol	1.3	± 0.3	0.4	1.1	± 0.3	0.3	1.4	± 0.2	0.4	0.9	± 0.4	0.4	<b>0.02</b>	± 0.0	<b>0.1</b>
Unknowns															
Total (10 to 2 $\mu\text{g}\cdot\text{cm}^{-2}$ of cuticle)	324.4	± 23.1		321.8	± 33.48		361.0	± 26.6		220.2	± 84.4		<b>38.0</b>	± 7.9	

Quantifications are means of four replicates  $\pm$  sd. Bold values represent significant differences from the wild type (*t* test,  $P < 0.05$ ). nd, below the detection limit. Third column represents the percentage of each compound related to the total cutin monomer or total wax compound contents.

Higher magnification AFM images of cutin isolated from 20-DPA fruits show an amorphous smooth surface with regular structure, including some nodules-structure from 20 to 80 nm as previously described (Round et al., 2000; Benítez et al., 2004) (Figure 7). The calculated root mean squared roughness parameter ranged from 7 to 12 nm at 20 DPA. This parameter appears to be approximately invariant for all of the RNAi lines. Nevertheless, nanopores with a mean diameter of  $\sim$ 20 nm were observed on the cutin surfaces of some 20-DPA fruits of L-17. These irregularly distributed nanopores indicate a defect in the continuity of the cutin structure, as highlighted by the TB test,

and are probably related to modifications of the polymerization process, as suggested by ATR-FTIR data (Figure 6C).

## DISCUSSION

### GDSL1 Is an Extracellular Protein Primarily Involved in Cutin Deposition

From the synthesis of cutin monomers (i.e., hydroxy-fatty acids) and cutin building blocks (either monoglycerides or oligomers) to the translocation in the apoplast compartment through ABC

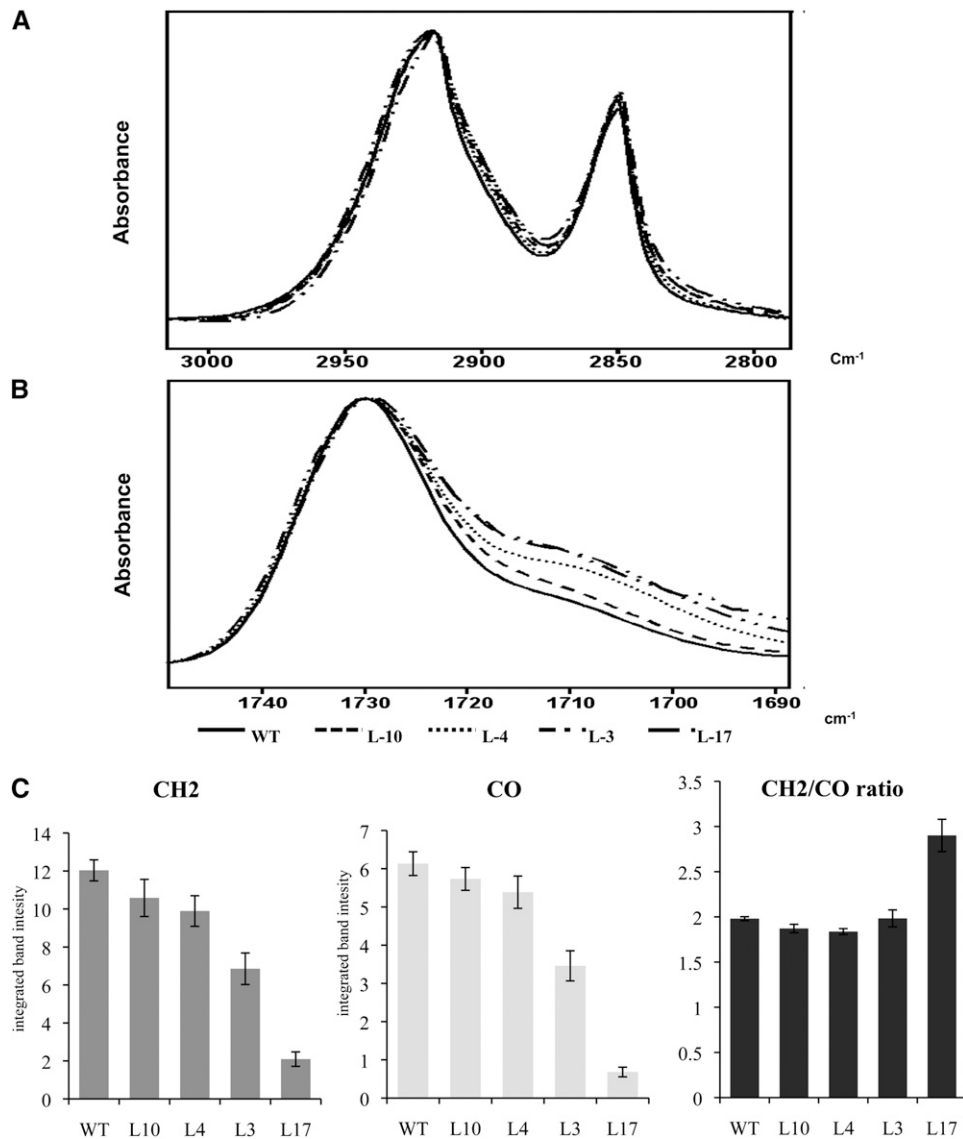


**Figure 6.** FTIR Analyses of Isolated Cutin of Breaker + 7 d Fruits from Wild-Type and P35S-SIGDSL1 RNAi Plants.

Normalized cutin spectra are representative of identical spectra obtained from four biological replicates.

**(A)** Focus on spectra region corresponding to the methylene vibrations.

**(B)** Focus on spectra region corresponding to carbonyl vibrations. WT, the wild type.

**(C)** Surfaces of CH<sub>2</sub> (2978 to 2838 cm<sup>-1</sup>) and CO (1750 to 1690 cm<sup>-1</sup>) bands and the ratio of CH<sub>2</sub>/CO areas of wild-type and RNAi lines. Mean values ( $\pm$ sd) are calculated from non-normalized surfaces and from eight replicates from four biological replicates.

transporters (Pollard et al., 2008; Yang et al., 2010), much progress has recently been made in delineating the intricate pathway leading to cutin deposition. In this research area, the black box remains the mechanisms of extracellular polymerization of cutin. The three-dimensional structure of the cutin polyester is still unknown, and solid state NMR techniques have provided only limited information on the dynamics (Zlotnik-Mazori and Stark, 1988; Round et al., 2000) and cross-linking of cutin polyesters (Fang et al., 2001; Deshmukh et al., 2003). Genetic approaches based on the identification of mutant plants exhibiting cuticular defects or on reverse genetics analysis of

candidate genes are promising but, to date, have provided only limited characterization of the extracellular assembly of cutin polyesters.

In this article, we demonstrate that an extracellular protein of the ubiquitous plant GDSL-lipase family (i.e., *S. lycopersicum* GDSL1) affects cutin deposition. Several lines of evidence reported here support this role. First, in the tomato fruit, GDSL1 is expressed in the exocarp of developing fruits (Figure 1). Second, proteomic analysis and immunolabeling showed that GDSL1 is embedded in the extracellular cutinized matrix of fruit cuticles, while it is absent from the noncutinized cell wall (Figure 5). Third,

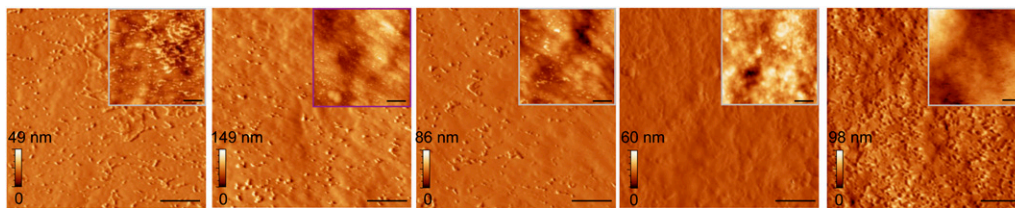


**Figure 7.** Fine AFM Images of Tomato Fruit Cutin Surface of Wild-Type and RNAi Transgenic Lines at 20 DPA.

Images were taken in tapping mode at  $2 \times 2\text{-}\mu\text{m}$  magnification. Error signal and topographical signal (in inset) are presented. Bars = 400 nm. [See online article for color version of this figure.]

we observed that the extent of the alterations of cutin deposition (i.e., cuticle thickness, cutin monomer contents, cutin monomer composition, and cutin density, considered here as the cutin monomer to cutin-associated cell wall ratio) is closely related to the severity of *GDSL1* silencing. In addition, *GDSL1* silencing did not lead to pleiotropic effects and the cuticle appears to be the primary affected target. However, the wax load of transgenic fruit cuticles was significantly impacted only when the expression of *GDSL1* was severely reduced and this likely represents a secondary effect.

A biological role of GDSL-lipases in cutin deposition is in agreement with previous data showing that these proteins are localized to the apoplastic space of seedlings (Takahashi et al., 2010; Teutschbein et al., 2010) or to the epidermis of leaves and fruits (Reina et al., 2007; Matas et al., 2010; Yeats et al., 2010). Although the structure and composition of cutin were not characterized, the cosilencing of two *Arabidopsis* GDSL-lipases led to severe floral organ fusion and major changes in the architecture of epidermis cells (Shi et al., 2011). The cuticular localization of GDSL1 also fits perfectly with the role of these proteins in mediating the plant's tolerance to biotic and abiotic stress (Oh et al., 2005; Naranjo et al., 2006; Hong et al., 2008). Indeed, cutin is recognized as a physical barrier as well as a source of signaling molecules that regulate the dialog between plants and their environment (Kolattukudy, 2001; Reina-Pinto and Yephremov, 2009).

It has been shown (Park et al., 2010) that the rice (*Oryza sativa*) T-DNA insertional *wdl1* mutant, which exhibits increased water loss, was affected in the expression of a GDSL-lipase-like gene. However, WDL1 is only distantly related to the canonical plant GDSL-lipases and shows poor conservation of the invariant blocks I, II, and V. In particular, the GDSL motif, localized in block I, is replaced by glycine-serine-serine-isoleucine. Furthermore, this motif, which is involved in the catalytic triad of the GDSL-lipase family (Ling et al., 2006), is predicted to be localized to the putative signal peptide (SignalP and TargetP software). Finally, in contrast with GDSL1, WDL1 deficiency does not impact the cutin monomer content but leads to irregular cuticle deposition as well as to cell wall modifications.

It should be emphasized here that GDSL-lipases form a large multigenic family of plant proteins that are divided into three subfamilies (Volokita et al., 2011). The extremely conserved GDSL-motif and the highly conserved domains are not sufficient criteria for an ab initio prediction of the function of the protein. In support of such an assertion, one can mention that the maize (*Zea mays*) acetylcholine esterase, *Brassica napus* sinapine

esterase, and the chlorogenate:glucarate caffeoyltransferase of tomato seedlings share the same GDSL motif and the five conserved domains with GDSL1 (Sagane et al., 2005; Clauss et al., 2008; Teutschbein et al., 2010).

### The *GDSL1*-Silenced Lines Do Not Display Pleiotropic Phenotypic Alterations

Many *Arabidopsis* cutin mutants, such as *bdg*, *fdh*, *lcr*, and *dcr* (Pruitt et al., 2000; Wellesen et al., 2001; Kurdyukov et al., 2006b; Bird et al., 2007; Panikashvili et al., 2009), exhibit pleiotropic phenotypes, including organ fusion, abnormal development, or deformation of epidermal cells accompanied by distorted deposition of cutin polymer. Remarkably, the drastic (98%) reduction in *GDSL1* expression and the corresponding decrease in cuticle thickness do not compromise fruit growth and development and do not induce any visible modification of the epidermal cell morphology.

Furthermore, in contrast with *Arabidopsis* mutants affected in the expression of cutin-specific ABC transporters (Bird et al., 2007; Bessire et al., 2011), we did not observe any accumulation of lipid inclusions and lamellar bodies in epidermis cells. This agrees with our analysis of the expression of some candidate genes of the cutin biosynthesis pathway. Indeed, the significant downregulation of oxidase genes (i.e., *HOTHEAD-like* and *CYP86A7-like* genes) and *GPAT4* and *GPAT6-like* genes indicates a possible feedback regulation that could prevent epidermis cells from accumulating potentially toxic cutin monomers and precursors.

Only changes in cuticle permeability to hydrophilic molecules (TB) and increased postharvest water loss were observed in P35S-SIGDSL1 RNAi lines. The permeance properties of tomato cuticles were mostly affected in line L-17, where AFM images and ATR-FTIR analysis highlighted defects in cutin assembly. However, these defects are probably not sufficient to lead to major developmental abnormalities, like those observed in the *Arabidopsis* cutin mutants. This suggests that a 2% residual expression of GDSL1 provides a sufficient level of enzyme to sustain fruit development. However, at this stage, we cannot exclude the possibility that a more stringent *GDSL1* silencing or a null mutation might trigger pleiotropic alterations and impair fruit development. Nevertheless, these results also indicate that tomato can afford a huge reduction in the thickness of fruit cuticle, as long as the cutin is homogeneously deposited. Such a conclusion is in full agreement with the characterized tomato cutin deficiency mutants *cd1*, *cd2*, and *cd3*, in which a 95%

reduction in cutin thickness does not impact either fruit growth or the postharvest water loss in the case of the *cd2* and *cd3* mutants (Isaacson et al., 2009).

### Potential Mechanisms Relating GDSL1 to Extracellular Cutin Deposition

The impact of GDSL1 deficiency on cutin deposition raises the question of how this extracellular enzyme could operate in planta. Plant GDSL-lipases are generally depicted as acyl-hydrolases (Abdelkafi et al., 2009; Updegraff et al., 2009). Their hydrolytic activity has been widely associated with seed germination (Clauss et al., 2008), pollen hydration (Updegraff et al., 2009), pathogen defense (Oh et al., 2005; Kwon et al., 2009; Lee et al., 2009a), and the abiotic stress response (Hong et al., 2008; Zhou et al., 2009). In the P35S-SIGDSL1 RNAi plants, both AFM analyses (showing the presence of nanopores) and FTIR spectra (indicating a lower polymerization index) support a potential polymerase activity of GDSL1. The acyl-hydrolase activity of plant GDSL-lipases is based on *in vitro* assays performed with recombinant proteins in diluted aqueous solutions, far from their genuine biological context. Actually, the localization of GDSL1 in the cuticle matrix and not in the cell walls shows that the protein operates in a peculiar hydrophobic environment. It is known that lipases are active in water-depleted organic solvents (Klibanov, 2001) and can catalyze the polyesterification of hydroxy-fatty acids in such conditions (Mahapatro et al., 2004; Ebata et al., 2007). Moreover, the extent of polymerization is improved when the lipase is immobilized on an acrylic resin (Ebata et al., 2007). The ester precursors of the transesterification process could be the monoglycerides produced by specific intracellular GPATs (Yang et al., 2010) or oligomers (Panikashvili et al., 2011). The monoglycerides are secreted in the apoplastic compartment (Li et al., 2007a) and small lipid molecules, monoglycerides, and oligomers are compatible with the involvement of ABC transporters in cutin deposition (Bird, 2008). These putative substrates of GDSL-lipase also fit well with previous data indicating that esters are more convenient substrates than free fatty acids for the acyl-transfer activity in a hydrophobic context (Ebata et al., 2007). Therefore, the immobilization of GDSL1 in the cutin matrix, a water-depleted hydrophobic environment, can favor the reverse reaction of this lipase (i.e., transesterification activity of ester precursors). It was recently established, *in vitro*, that CD1 protein, identical to GDSL1, is endowed with acyltransferase activity and that 2-mono-(10,16-dihydroxyhexadecanoyl)-glycerol is a substrate for this enzyme (Yeats et al., 2012). This acyltransferase activity supports our major conclusion that GDSL1 plays an essential role in the process of cutin deposition during fruit cuticle development.

However, in planta, we also have to consider that GDSL1 can exhibit both hydrolase and transferase activities. Indeed, a plant GDSL-lipase involved in pyrethrins biosynthesis harbors transferase activity *in vivo* and esterase activity *in vitro* (Kikuta et al., 2012). Such dual activities are also observed *in vivo* in the case of enzymes involved in cell wall assembly. Indeed, xyloglucan endotransglucosylase/hydrolase (XTH) form a multigenic family in which some XTH can display both hydrolase and transferase activities (Rose et al., 2002). These catalytic specificities are

related to subtle structural modifications (Eklöf and Brumer, 2010). Different XTHs are expressed during organ development or upon environmental stress, processes that involve cell wall remodeling (Rose et al., 2002). In this regard, it was recently shown that the ectopic overexpression of a pollen GDSL-lipase CDEF1 in the vegetative organs of *Arabidopsis* disrupts the cuticle (Takahashi et al., 2010) in a manner similar to *cute* mutants expressing a fungal cutinase (Sieber et al., 2000). This apparent contradiction between GDSL1 and CDEF1 activities strengthens our hypothesis that GDSL-lipases could have hydrolase or transferase activities, depending on whether they are present in the cell wall or aqueous apoplast, as observed for CDEF1, or in the hydrophobic cuticle, as shown here for GDSL1.

All our experimental data converge toward a key role of GDSL-lipase in the extracellular polymerization and/or cross-linking of the cutin polyester. However, cutin is a complex polyester that includes lipids, glycerol, and aromatics and is anchored to cell wall polysaccharides. Therefore, we cannot exclude the possibility that GDSL1 is involved in the cross-linking between cutin and the cell wall. In this regard, it was reported that TBL (for Trichome birefringence-like) genes containing a GDSL motif are involved in the esterification of pectic polymers within cellulose in *Arabidopsis* trichomes (Bischoff et al., 2010). In addition, a GDSL-lipase was involved in the esterification of phenolic compounds, which are minor compounds of the cuticle, in the apoplastic compartment of tomato seedlings (Teutschbein et al., 2010). To delineate this sophisticated enzymatic process, including the identification of substrates and potential protein partners, *in vitro* and biomimetic devices have to be designed. Conceivably, different extracellular acyltransferases may be required to catalyze the multiple cross-links present in the cuticular matrix. Moreover, it has been shown that different GDSL-lipases are expressed in the epidermis during the growth of tomato fruits (Yeats et al., 2010). GDSL1 is undoubtedly an element of a complex network required for the establishment of the plant cuticle. In this regard, the *GDSL1*-silenced plants provide a powerful tool to further investigate the genetic and metabolic networks underlying plant cuticle formation.

## METHODS

### Plant Material and Growth Conditions

Transcript analyses of fruit tissues and proteome experiments were performed on *Solanum lycopersicum* 'Ailsa Craig' grown as previously described (Mounet et al., 2009). A cherry tomato variety was used to generate transgenic plants (*S. lycopersicum* 'West Virginia 106'). *In vitro* culture and growth of transgenic plants were performed as previously indicated (Alhagdow et al., 2007).

### Plant Transformation

The GDSL1 cDNA fragment was obtained by reverse transcription (SuperScript II reverse transcriptase; Invitrogen, Life Technology) of 2 µg of total RNA from tomato fruit. A fragment of 509 bp, located in the 5'-region of *GDSL1*, was amplified by PCR using ExTaq DNA polymerase and the gene-specific primers 5'-AAAAGCAGGCTTTTTTGTGCTAATTTTTGCCTA-3' and 5'-AGAAAGCTGGGTCAACAATATCCACACTCCACCCTA-3', where the underlined sequence corresponds to partial attB extensions.

After a second PCR using full attB primers (attB1, 5'-GGGGACAA-GTTTGTACAAAAAGCAGGCT-3'; attB2, 5'-GGGGACCACTTTGTA-CAAGAAAGCTGGGT-3'), the purified DNA fragment was introduced in the Gateway system entry vector (pDONR 201) and then transferred as an inverted repeat under the control of the 35S promoter in the RNAi destination vector (pK7GWIWG2), which confers kanamycin resistance to transformed plants (Karimi et al., 2007). After sequence checking, constructions were used to transform cherry tomato plants ('West Virginia 106') via *Agrobacterium tumefaciens* strain GV3101 (Hamza and Chupeau, 1993). Homozygous T2 plants were used for all of the analyses.

### Isolation of Tomato Fruit Cuticles

Cuticles were isolated from the fruits of wild-type and transgenic lines according to a previously described protocol (Schönherr and Riederer, 1986). Cutin was obtained after subsequent dewaxing by immersion in methylene chloride and repeated three times. Purified cutin slices were scanned and their surface was assessed using Image J software (<http://rsb.info.nih.gov/ij/>).

### Phenotypic Characterization of Fruit from Wild-Type and Transgenic Lines

Red ripe fruits (breaker + 7 d) from wild-type and P35S-SIGDSL1 RNAi transgenic lines were harvested and submitted to L\*a\*b\* analyses using a Minolta CR-200 chromameter (Clarys et al., 2000). Mean values for the L\*, which correspond to luminance character, were obtained by three measurements in the equatorial zone of 16 fruits for each line. A desiccation tolerance test, through weight loss measurement, was performed by incubating the fruits at 30°C for 21 d. Finally, a TB assay was performed to identify defects in the permeability of fruit cuticles (Tanaka et al., 2004; Hovav et al., 2007).

For cuticle thickness measurements, the fruit pericarp (including cuticle) was obtained from three independent fruits (breaker + 7) of wild-type and P35S-SIGDSL1 RNAi transgenic lines. Samples were fixed and embedded in paraffin as previously described (Bereterbide et al., 2002). Ten-micrometer slices of pericarp were stained using saturated and filtered Sudan Red solution in ethanol. Mean cutin thickness was assessed from 60 measurements.

For auramine O staining, paraffin-embedded exocarp of 20-DPA wild-type fruits were stained according to Buda et al. (2009) and were observed through an A1 Nikon confocal laser scanning microscope with a  $\times 40$  water immersion objective. Excitation was conducted by a light-emitting diode at 485 nm, and emission was collected between 400 and 718 nm. The resulting images were acquired, stored, and visualized with a Nikon NIS-Elements software program

### Proteomic Analysis of Tomato Fruit Cutin

Cutin powder was suspended in 5 volumes of 0.5 M NaCl and 1 mM phenylmethylsulfonyl fluoride overnight at room temperature and sonicated (24 W, 15 min). After dialysis (cutoff of 3500 D), the protein extract was freeze-dried and analyzed by one-dimensional SDS-PAGE. Protein bands were excised and subjected to trypsin digestion before liquid chromatography coupled to tandem mass spectrometry (Perrocheau et al., 2005). Protein identification was performed by comparing the tandem mass spectrometry sequence with the Swiss-prot (<http://www.ebi.ac.uk/uniprot/>) and TIGR EST (<http://plantta.jcvi.org/>) databases.

### ATR-FTIR and AFM

FTIR spectra (200 scans) were recorded at a resolution of 2  $\text{cm}^{-1}$  on a Nicolet Magna IR 550 spectrometer equipped with a liquid nitrogen-cooled mercury-cadmium-telluride detector. The instrument was continuously purged with dry air. Spectra of cutin films were obtained by ATR

using a single reflection accessory fitted with a thermostated diamond crystal with a 45° angle of light incidence. Two spectra were acquired on four different parts of the fruit cutin, and four fruits per line were analyzed. Surface calculations were conducted from the non-normalized spectra after baseline correction, which was established in the same conditions through Galactic software (Thermo Scientific). The surfaces of  $\text{CH}_2$  (2978 to 2838  $\text{cm}^{-1}$ ) and CO (1750 to 1695  $\text{cm}^{-1}$ ) bands were measured and used to calculate the ratio  $R_{\text{CH}_2/\text{CO}}$ .

AFM height, phase, and error-signal images of isolated cutins were acquired in air using an Autoprobe CP Park Scientific Instrument. AFM images were recorded in the tapping mode using conventional pyramidal silicon nitride cantilevers obtained from Digital Instruments. All the tapping mode images were acquired at the lowest possible stable scanning force (<10 nN). Different surface areas were scanned for each sample, from 80  $\mu\text{m} \times 80 \mu\text{m}$  to 2  $\mu\text{m} \times 2 \mu\text{m}$ . At least three fruits from each wild-type and P35S-SIGDSL1 RNAi transgenic line were used for the 80  $\times$  80- $\mu\text{m}$  scans, and the 2  $\times$  2- $\mu\text{m}$  AFM image was taken at two different locations for each sample. The mean surface roughness, which was calculated from the root mean square roughness, was deduced from the 2  $\times$  2- $\mu\text{m}^2$  height images.

### Wax and Cutin Monomer Analyses

Cuticular waxes were extracted from isolated cuticles of three tomato fruits in 6 mL of methylene chloride and analyzed as previously described (Kurdyukov et al., 2006b). Overnight cutin depolymerization was performed with 14%  $\text{BF}_3$  in methanol (Sigma-Aldrich), and 10  $\mu\text{g}$  heptadecanoic acid was used as the internal standard (Osman et al., 1999). After extraction with methylene chloride, methylated cutin monomers were silylated with bis-(trimethylsilyl) trifluoroacetamide containing 1% trimethylchlorosilane (Sigma-Aldrich). Exocarp lipids were extracted by hexane/isopropanol (3:2) and were either directly silylated or trans-methylated in methanol/ $\text{BF}_3$  before silylation. Lipids were analyzed by gas chromatography-mass spectrometry (Thermo DSQII; 70 eV, mass-to-charge ratio of 50 to 700) and gas chromatography-flame ionization detection (Hewlett Packard 5890) using identical columns (DB5ms; 30 m  $\times$  0.25 mm, 0.1 mm [JandW]) and temperature gradients.

### Production of Recombinant GDSL1 for Generation of Polyclonal Antibodies

Recombinant GDSL1 was produced in *Escherichia coli* (Origami) as previously described (Elmorjani et al., 2004; de Zélicourt et al., 2007) after amplification using specific primers (*GDSL3'*, 5'-TAAAGCTTATGCATG-TGAAT-3'; and *GDSL5'*, 5'-ATCCATGGGGCAAAGTGAAGCTAGGGC-ATTT-3') and insertion into expression vectors.

Recombinant GDSL1 was extracted in a buffer containing 8 M urea and further purified by  $\text{Ni}^{2+}$  affinity chromatography. Urea was removed by extensive dialysis against a 50 mM Tris-HCl and 200 mM NaCl, pH 7.5, buffer. This led to the aggregation of the purified protein. After centrifugation at 10,000g, the protein pellet was suspended in Freund's adjuvant for immunization. Antibody production was conducted according to Dubreil et al. (2002). The specificity of polyclonal antibodies was tested by immunoblotting and indirect capture ELISA. For immunoblot analysis, total protein was extracted from 50 mg fruit pericarps ground in liquid nitrogen and then washed twice with a methylene chloride/methanol (2:1) solution. Proteins were extracted with 50 mM Tris-HCl buffer, pH 8.0, 2% SDS, and 1% mercaptoethanol. After electroblotting, SIGDSL1 was revealed using the Immuno-Star AP kit (Bio-Rad).

### Immunocytochemical Localization of GDSL1

Fruit exocarp (including cuticle) was collected from three independent 20-DPA fruits from wild-type and P35S-SIGDSL1 RNAi L-3 and L-17 lines

and fixed as previously described (Guillon et al., 2011). Thin ultramicrotome sections (Micom RMC MT 700) of either 1  $\mu\text{m}$  for confocal laser scanning microscopy or 100 nm for electron microscopy were obtained.

For nanogold immunolabeling, sections of tomato exocarp from wild-type, P35S-SIGDSL1 L-3, and L-17 fruits were incubated in 3% (w/v) BSA in 10 mM PBS (pH 7.2) and incubated for 1 h with the polyclonal antibody diluted in 10 mM PBS supplemented with 1% BSA and 0.05% Tween 20. After extensive washing, the section was incubated for 1 h with secondary antibodies conjugated with goat anti-rabbit 1-nm colloidal gold complexes (Aurion). Labeling was intensified through the use of a silver enhancement kit (Aurion) according to the manufacturer's instructions. After washing, the grids were stained with 2% uranyl acetate. Electrographs were taken with a Jeol 100S TEM electron microscope. In control experiments, preimmune serum was used (see Supplemental Figure 8 online).

For fluorescence immunolabeling, 1- $\mu\text{m}$  exocarp sections were saturated with 0.01 M Na-PBS, pH 7.2, containing 4% fat-free milk powder (PBS milk) during the 30 min prior to incubation for 1 h with polyclonal antibodies (1:100). After extensive washing in PBS, the sections were incubated for 1 h with the goat anti-rabbit IgG coupled to Alexa Fluor-546 (1:100; Molecular Probes, Invitrogen). Immunostained sections were then thoroughly washed in PBS and deionized water and mounted in deionized water to be visualized by fluorescence. The immunofluorescence sections were analyzed by an A1 Nikon confocal laser scanning microscope with a  $\times 40$  water immersion objective. Excitation was conducted by a light-emitting diode at 561 nm, and emission was collected between 570 and 620 nm. The resulting images were acquired, stored, and visualized with the Nikon NIS-Elements software program.

#### Real-Time RT-PCR

For measurement of *GDSL1* transcript level in fruit tissues, the seed, locular tissue, columella, mesocarp, and exocarp were separated from 20-DPA 'Ailsa Craig' fruit, ground in liquid nitrogen, and stored at  $-80^{\circ}\text{C}$  until RNA extraction, as described previously (Mounet et al., 2009). The exocarp sample represents the entire tomato peel, comprising the cuticle, epidermal cells, and a few layers of collenchyma cells. For each wild-type and P35S-SIGDSL1 RNAi line ('WVa 106' cultivar), measurements of *GDSL1* transcript levels were performed on pools of fruit. Total RNA was isolated, treated with DNase, and reverse transcribed as previously described (Mounet et al., 2009).

PCR primers were designed in the 3' untranslated region and are available in Supplemental Table 1 online. Real-time PCR was performed on a Bio-Rad CFX96 real-time system with the following parameters: denaturation at  $95^{\circ}\text{C}$  for 90 s, 40 amplification cycles with a denaturation step at  $95^{\circ}\text{C}$  for 30 s, and a hybridization/synthesis step at  $60^{\circ}\text{C}$  for 30 s. Data acquisition and analysis were done using the Bio-Rad CFX Manager software (version 1.1.308.1111). *Eif4 $\alpha$*  (BT013166),  $\beta$ -*tubulin* (DQ205342), and *actin* (SGN-U213132), based on de Jong et al., (2009), were used as housekeeping genes to calculate relative transcript expression using gene expression analysis for the iCycler IQ real-time PCR detection system. A Student's *t* test was performed using the mean value and sd of four replicates.

#### Accession Numbers

Sequence data from this article can be found in the SOL Genomics Network (<http://www.sgn.cornell.edu/>) under the following accession number: GDSL1, SGN-U585129.

#### Supplemental Data

The following materials are available in the online version of this article.

**Supplemental Figure 1.** Expression Pattern of SI *GDSL1* in Ailsa Craig Fruit Tissues.

**Supplemental Figure 2.** Nucleotide and Deduced Protein Sequences of SI *GDSL1*.

**Supplemental Figure 3.** Localization of SI *GDSL1* in 20-DPA Tomato Fruit Cuticle.

**Supplemental Figure 4.** Ultrastructural Feature of Epidermal Cells of Cutinized Exocarps.

**Supplemental Figure 5.** Transcript Levels of Cutin-Associated Genes in Wild-Type and P35S-SIGDSL1 RNAi Transgenic Lines.

**Supplemental Figure 6.** Total ATR-FTIR Spectra.

**Supplemental Figure 7.** AFM Images of Tomato Cutin Surfaces of Fruits from Wild-Type and P35S-SIGDSL1 RNAi Plants at 20 DPA and Breaker + 7 d Stages.

**Supplemental Figure 8.** Immunolabeling of Tomato Exocarp with Preimmune Sera.

**Supplemental Table 1.** Accession and Sequence Information Concerning Real-Time RT PCR Primers.

#### ACKNOWLEDGMENTS

We thank André Lelion and Nathalie Geneix for their excellent technical expertise. We thank Brigitte Bouchet for help with TEM analyses, Michele Viau for assistance with gas chromatography analysis, and Marc Lahaye for constructive discussion on the article. This work was supported by the French Ministry of Research (A.-L.G.) and Institut National de la Recherche Agronomique Department Caracterisation et Elaboration des Produits Issus de l'Agriculture (F.M.).

#### AUTHOR CONTRIBUTIONS

M.L.-C., C.R., D.M., and B.B. designed the research. A.-L.G., F.M., C.G., M.L.-C., V.G., J.V., J.-L.R., B.Q., K.E., J.P., V.G., and B.B. performed the experiments. A.-L.G., F.M., C.G., M.L.-C., B.Q., K.E., C.R., D.M., and B.B. analyzed the data. M.L.-C., K.E., C.R., D.M., and B.B. wrote the article.

Received May 29, 2012; revised May 29, 2012; accepted June 26, 2012; published July 17, 2012.

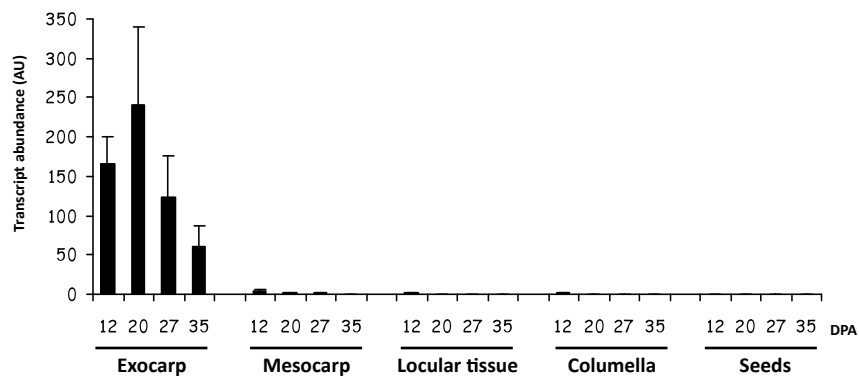
#### REFERENCES

- Abdelkafi, S., Ogata, H., Barouh, N., Fouquet, B., Lebrun, R., Pina, M., Scheirlinckx, F., Villeneuve, P., and Carrière, F. (2009). Identification and biochemical characterization of a GDSL-motif carboxylester hydrolase from *Carica papaya* latex. *Biochim. Biophys. Acta* **1791**: 1048–1056.
- Aharoni, A., Dixit, S., Jetter, R., Thoenes, E., van Arkel, G., and Pereira, A. (2004). The SHINE clade of AP2 domain transcription factors activates wax biosynthesis, alters cuticle properties, and confers drought tolerance when overexpressed in *Arabidopsis*. *Plant Cell* **16**: 2463–2480.
- Akoh, C.C., Lee, G.C., Liaw, Y.C., Huang, T.H., and Shaw, J.F. (2004). GDSL family of serine esterases/lipases. *Prog. Lipid Res.* **43**: 534–552.
- Alhagdow, M., Mounet, F., Gilbert, L., Nunes-Nesi, A., Garcia, V., Just, D., Petit, J., Beauvoit, B., Fernie, A.R., Rothan, C., and Baldet, P. (2007). Silencing of the mitochondrial ascorbate synthesizing enzyme L-galactono-1,4-lactone dehydrogenase affects plant and fruit development in tomato. *Plant Physiol.* **145**: 1408–1422.

- Beisson, F., Li, Y., Bonaventure, G., Pollard, M., and Ohlrogge, J.B. (2007). The acyltransferase GPAT5 is required for the synthesis of suberin in seed coat and root of *Arabidopsis*. *Plant Cell* **19**: 351–368.
- Benítez, J.J., Matas, A.J., and Heredia, A. (2004). Molecular characterization of the plant biopolyester cutin by AFM and spectroscopic techniques. *J. Struct. Biol.* **147**: 179–184.
- Bereterbide, A., Hernould, M., Farbos, I., Glimelius, K., and Mouras, A. (2002). Restoration of stamen development and production of functional pollen in an alloplasmic CMS tobacco line by ectopic expression of the *Arabidopsis thaliana* SUPERMAN gene. *Plant J.* **29**: 607–615.
- Bessire, M., Borel, S., Fabre, G., Carraça, L., Efremova, N., Yephremov, A., Cao, Y., Jetter, R., Jacquat, A.-C., Métraux, J.-P., and Nawrath, C. (2011). A member of the PLEIOTROPIC DRUG RESISTANCE family of ATP binding cassette transporters is required for the formation of a functional cuticle in *Arabidopsis*. *Plant Cell* **23**: 1958–1970.
- Bessire, M., Chassot, C., Jacquat, A.C., Humphry, M., Borel, S., Petétot, J.M., Métraux, J.P., and Nawrath, C. (2007). A permeable cuticle in *Arabidopsis* leads to a strong resistance to *Botrytis cinerea*. *EMBO J.* **26**: 2158–2168.
- Bird, D., Beisson, F., Brigham, A., Shin, J., Greer, S., Jetter, R., Kunst, L., Wu, X., Yephremov, A., and Samuels, L. (2007). Characterization of *Arabidopsis* ABCG11/WBC11, an ATP binding cassette (ABC) transporter that is required for cuticular lipid secretion. *Plant J.* **52**: 485–498.
- Bird, D.A. (2008). The role of ABC transporters in cuticular lipid secretion. *Plant Sci.* **174**: 563–569.
- Bischoff, V., Nita, S., Neumetzler, L., Schindelasch, D., Urbain, A., Eshed, R., Persson, S., Delmer, D., and Scheible, W.R. (2010). TRICHOME BIREFRINGENCE and its homolog AT5G01360 encode plant-specific DUF231 proteins required for cellulose biosynthesis in *Arabidopsis*. *Plant Physiol.* **153**: 590–602.
- Blee, E., and Schubert, F. (1993). Biosynthesis of cutin monomers: Involvement of a lipoxygenase/peroxygenase pathway. *Plant J.* **4**: 113–123.
- Blein, J.P., Coutos-Thévenot, P., Marion, D., and Ponchet, M. (2002). From elicitors to lipid-transfer proteins: A new insight in cell signalling involved in plant defence mechanisms. *Trends Plant Sci.* **7**: 293–296.
- Blume, A., Hübner, W., and Messner, G. (1998). Fourier transform infrared spectroscopy of  $^{13}\text{C}$  = O-labeled phospholipids hydrogen bonding to carbonyl group. *Biochemistry* **27**: 8239–8249.
- Buda, G.J., Isaacson, T., Matas, A.J., Paolillo, D.J., and Rose, J.K. (2009). Three-dimensional imaging of plant cuticle architecture using confocal scanning laser microscopy. *Plant J.* **60**: 378–385.
- Chen, G. et al. (2011). An ATP-binding cassette subfamily G full transporter is essential for the retention of leaf water in both wild barley and rice. *Proc. Natl. Acad. Sci. USA* **108**: 12354–12359.
- Clarys, P., Alewaeters, K., Lambrecht, R., and Barel, A.O. (2000). Skin color measurements: comparison between three instruments: The Chromameter(R), the DermaSpectrometer(R) and the Mexameter(R). *Skin Res. Technol.* **6**: 230–238.
- Clauss, K., Baumert, A., Nimtz, M., Milkowski, C., and Strack, D. (2008). Role of a GDLS lipase-like protein as sinapine esterase in *Brassicaceae*. *Plant J.* **53**: 802–813.
- Croteau, R., and Kolattukudy, P.E. (1973). Enzymatic synthesis of a hydroxy fatty acid polymer, cutin, by a particulate preparation from *Vicia faba* epidermis. *Biochem. Biophys. Res. Commun.* **52**: 863–869.
- Croteau, R., and Kolattukudy, P.E. (1974). Biosynthesis of hydroxy-fatty acid polymers. Enzymatic synthesis of cutin from monomer acids by cell-free preparations from the epidermis of *Vicia faba* leaves. *Biochemistry* **13**: 3193–3202.
- da Luz, B.R. (2006). Attenuated total reflectance spectroscopy of plant leaves: A tool for ecological and botanical studies. *New Phytol.* **172**: 305–318.
- D'Auria, J.C. (2006). Acyltransferases in plants: A good time to be BAHD. *Curr. Opin. Plant Biol.* **9**: 331–340.
- Deshmukh, A.P., Simpson, A.J., and Hatcher, P.G. (2003). Evidence for cross-linking in tomato cutin using HR-MAS NMR spectroscopy. *Phytochemistry* **64**: 1163–1170.
- Douliez, J.P., Michon, T., and Marion, D. (2000). Structure, biological and technological functions of lipid transfer proteins and indolines, the major lipid binding proteins from cereal kernels. *J. Cereal Sci.* **32**: 1–20.
- de Zélicourt, A., Letousey, P., Thoiron, S., Campion, C., Simoneau, P., Elmorjani, K., Marion, D., Simier, P., and Delavault, P. (2007). Ha-DEF1, a sunflower defensin, induces cell death in *Orobanche* parasitic plants. *Planta* **226**: 591–600.
- Dubreil, L., Biswas, S.C., and Marion, D. (2002). Localization of puroindoline-a and lipids in bread dough using confocal scanning laser microscopy. *J. Agric. Food Chem.* **50**: 6078–6085.
- Ebata, H., Toshima, K., and Matsumura, S. (2007). Lipase-catalyzed synthesis and curing of high-molecular-weight polyricinoleate. *Macromol. Biosci.* **7**: 798–803.
- Eklöf, J.M., and Brumer, H. (2010). The XTH gene family: An update on enzyme structure, function, and phylogeny in xyloglucan remodeling. *Plant Physiol.* **153**: 456–466.
- Elmorjani, K., Lurquin, V., Lelion, A., Rogniaux, H., and Marion, D. (2004). A bacterial expression system revisited for the recombinant production of cystine-rich plant lipid transfer proteins. *Biochem. Biophys. Res. Commun.* **316**: 1202–1209.
- Fang, X., Qiu, F., Yan, B., Wang, H., Mort, A.J., and Stark, R.E. (2001). NMR studies of molecular structure in fruit cuticle polyesters. *Phytochemistry* **57**: 1035–1042.
- Graça, J., and Lamosa, P. (2010). Linear and branched poly(omega-hydroxyacid) esters in plant cutins. *J. Agric. Food Chem.* **58**: 9666–9674.
- Graça, J., Schreiber, L., Rodrigues, J., and Pereira, H. (2002). Glycerol and glyceryl esters of omega-hydroxyacids in cutins. *Phytochemistry* **61**: 205–215.
- Guillon, F., Bouchet, B., Jamme, F., Robert, P., Quémener, B., Barron, C., Larré, C., Dumas, P., and Saulnier, L. (2011). Brachypodium distachyon grain: Characterization of endosperm cell walls. *J. Exp. Bot.* **62**: 1001–1015.
- Hamza, S., and Chupeau, Y. (1993). Re-evaluation of conditions for plant regeneration and *Agrobacterium*-mediated transformation from tomato (*Lycopersicon esculentum*). *J. Exp. Bot.* **44**: 1837–1845.
- Heredia-Guerrero, J.A., San-Miguel, M.A., Sansom, M.S., Heredia, A., and Benítez, J.J. (2009). Chemical reactions in 2D: Self-assembly and self-esterification of 9(10),16-dihydroxypalmitic acid on mica surface. *Langmuir* **25**: 6869–6874.
- Hong, J.K., Choi, H.W., Hwang, I.S., Kim, D.S., Kim, N.H., Choi, S., Kim, Y.J., and Hwang, B.K. (2008). Function of a novel GDLS-type pepper lipase gene, CaGLIP1, in disease susceptibility and abiotic stress tolerance. *Planta* **227**: 539–558.
- Hovav, R., Chehanovsky, N., Moy, M., Jetter, R., and Schaffer, A.A. (2007). The identification of a gene (Cwp1), silenced during *Solanum* evolution, which causes cuticle microfissuring and dehydration when expressed in tomato fruit. *Plant J.* **52**: 627–639.
- Isaacson, T., Kosma, D.K., Matas, A.J., Buda, G.J., He, Y., Yu, B., Pravitarsari, A., Batteas, J.D., Stark, R.E., Jenks, M.A., and Rose, J.K. (2009). Cutin deficiency in the tomato fruit cuticle consistently affects resistance to microbial infection and biomechanical properties, but not transpirational water loss. *Plant J.* **60**: 363–377.
- Jeffree, C.E. (2006). The fine structure of the plant cuticle. In *Biology of the Plant Cuticle*, M.a.M.C. Riederer, ed (Oxford, UK: Blackwell), pp. 11–110.

- Jong, M., Mariani, C., and Vriezen, W.H.** (2009). The role of auxin and gibberellin in tomato fruit set. *J. Exp. Bot.* **60**: 1523–1532.
- Kannangara, R., Branigan, C., Liu, Y., Penfield, T., Rao, V., Mouille, G., Höfte, H., Pauly, M., Riechmann, J.L., and Broun, P.** (2007). The transcription factor WIN1/SHN1 regulates cutin biosynthesis in *Arabidopsis thaliana*. *Plant Cell* **19**: 1278–1294.
- Karimi, M., Depicker, A., and Hilson, P.** (2007). Recombinational cloning with plant gateway vectors. *Plant Physiol.* **145**: 1144–1154.
- Kikuta, Y., Ueda, H., Takahashi, M., Mitsumori, T., Yamada, G., Sakamori, K., Takeda, K., Furutani, S., Nakayama, K., Katsuda, Y., Hatanaka, A., and Matsuda, K.** (March 3, 2012). Identification and characterization of a GDSL lipase-like protein that catalyzes the ester-forming reaction for pyrethrin biosynthesis in *Tanacetum cinerariifolium*- A new target for plant protection. *Plant J.* <http://dx.doi.org/10.1111/j.1365-313X.2012.04980.x>.
- Klibanov, A.M.** (2001). Improving enzymes by using them in organic solvents. *Nature* **409**: 241–246.
- Kolattukudy, P.E.** (2001). Polyesters in higher plants. *Adv. Biochem. Eng. Biotechnol.* **71**: 1–49.
- Kram, B.W., Bainbridge, E.A., Perera, M.A., and Carter, C.** (2008). Identification, cloning and characterization of a GDSL lipase secreted into the nectar of *Jacaranda mimosifolia*. *Plant Mol. Biol.* **68**: 173–183.
- Kurdyukov, S., Faust, A., Nawrath, C., Bär, S., Voisin, D., Efremova, N., Franke, R., Schreiber, L., Saedler, H., Métraux, J.P., and Yephremov, A.** (2006b). The epidermis-specific extracellular BODYGUARD controls cuticle development and morphogenesis in *Arabidopsis*. *Plant Cell* **18**: 321–339.
- Kurdyukov, S., Faust, A., Trenkamp, S., Bär, S., Franke, R., Efremova, N., Tietjen, K., Schreiber, L., Saedler, H., and Yephremov, A.** (2006a). Genetic and biochemical evidence for involvement of HOTHEAD in the biosynthesis of long-chain alpha-, omega-dicarboxylic fatty acids and formation of extracellular matrix. *Planta* **224**: 315–329.
- Kusumawati, L., Imin, N., and Djordjevic, M.A.** (2008). Characterization of the secretome of suspension cultures of *Medicago* species reveals proteins important for defense and development. *J. Proteome Res.* **7**: 4508–4520.
- Kwon, S.J., Jin, H.C., Lee, S., Nam, M.H., Chung, J.H., Kwon, S.I., Ryu, C.M., and Park, O.K.** (2009). GDSL lipase-like 1 regulates systemic resistance associated with ethylene signaling in *Arabidopsis*. *Plant J.* **58**: 235–245.
- Lee, D.S., Kim, B.K., Kwon, S.J., Jin, H.C., and Park, O.K.** (2009a). *Arabidopsis* GDSL lipase 2 plays a role in pathogen defense via negative regulation of auxin signaling. *Biochem. Biophys. Res. Commun.* **379**: 1038–1042.
- Lee, S.B., Go, Y.S., Bae, H.J., Park, J.H., Cho, S.H., Cho, H.J., Lee, D.S., Park, O.K., Hwang, I., and Suh, M.C.** (2009b). Disruption of glycosylphosphatidylinositol-anchored lipid transfer protein gene altered cuticular lipid composition, increased plastoglobules, and enhanced susceptibility to infection by the fungal pathogen *Alternaria brassicicola*. *Plant Physiol.* **150**: 42–54.
- Leide, J., Hildebrandt, U., Reussing, K., Riederer, M., and Vogg, G.** (2007). The developmental pattern of tomato fruit wax accumulation and its impact on cuticular transpiration barrier properties: Effects of a deficiency in a beta-ketoacyl-coenzyme A synthase (LeCER6). *Plant Physiol.* **144**: 1667–1679.
- Lemaire-Chamley, M., Petit, J., Garcia, V., Just, D., Baldet, P., Germain, V., Fagard, M., Mouassite, M., Cheniclet, C., and Rothan, C.** (2005). Changes in transcriptional profiles are associated with early fruit tissue specialization in tomato. *Plant Physiol.* **139**: 750–769.
- Li, Y., Beisson, F., Koo, A.J., Molina, I., Pollard, M., and Ohlrogge, J.** (2007b). Identification of acyltransferases required for cutin biosynthesis and production of cutin with suberin-like monomers. *Proc. Natl. Acad. Sci. USA* **104**: 18339–18344.
- Li, Y., Beisson, F., Ohlrogge, J., and Pollard, M.** (2007a). Monoacylglycerols are components of root waxes and can be produced in the aerial cuticle by ectopic expression of a suberin-associated acyltransferase. *Plant Physiol.* **144**: 1267–1277.
- Li-Beisson, Y., Pollard, M., Sauveplane, V., Pinot, F., Ohlrogge, J., and Beisson, F.** (2009). Nanoridges that characterize the surface morphology of flowers require the synthesis of cutin polyester. *Proc. Natl. Acad. Sci. USA* **106**: 22008–22013.
- Ling, H.** (2008). Sequence analysis of GDSL lipase gene family in *Arabidopsis thaliana*. *Pak. J. Biol. Sci.* **11**: 763–767.
- Ling, H., Zhao, J., Zuo, K., Qiu, C., Yao, H., Qin, J., Sun, X., and Tang, K.** (2006). Isolation and expression analysis of a GDSL-like lipase gene from *Brassica napus* L. *J. Biochem. Mol. Biol.* **39**: 297–303.
- López-Casado, G., Matas, A.J., Domínguez, E., Cuartero, J., and Heredia, A.** (2007). Biomechanics of isolated tomato (*Solanum lycopersicum* L.) fruit cuticles: The role of the cutin matrix and polysaccharides. *J. Exp. Bot.* **58**: 3875–3883.
- Lü, S., Song, T., Kosma, D.K., Parsons, E.P., Rowland, O., and Jenks, M.A.** (2009). *Arabidopsis* CER8 encodes LONG-CHAIN ACYL-COA SYNTHETASE 1 (LACS1) that has overlapping functions with LACS2 in plant wax and cutin synthesis. *Plant J.* **59**: 553–564.
- Mahapatro, A., Kumar, A., and Gross, R.A.** (2004). Mild, solvent-free omega-hydroxy acid polycondensations catalyzed by *Candida antarctica* lipase B. *Biomacromolecules* **5**: 62–68.
- Mantsch, H.H., Madec, C., Lewis, R.N., and McElhaney, R.N.** (1987). Thermotropic phase behavior of model membranes composed of phosphatidylcholines containing di-methyl anteisobranched fatty acids. 2. An infrared spectroscopy study. *Biochemistry* **26**: 4045–4049.
- Matas, A.J., Agustí, J., Tadeo, F.R., Talón, M., and Rose, J.K.** (2010). Tissue-specific transcriptome profiling of the citrus fruit epidermis and subepidermis using laser capture microdissection. *J. Exp. Bot.* **61**: 3321–3330.
- Mintz-Oron, S., Mandel, T., Rogachev, I., Feldberg, L., Lotan, O., Yativ, M., Wang, Z., Jetter, R., Venger, I., Adato, A., and Aharoni, A.** (2008). Gene expression and metabolism in tomato fruit surface tissues. *Plant Physiol.* **147**: 823–851.
- Mounet, F., et al.** (2009). Gene and metabolite regulatory network analysis of early developing fruit tissues highlights new candidate genes for the control of tomato fruit composition and development. *Plant Physiol.* **149**: 1505–1528.
- Naranjo, M.A., Forment, J., Roldán, M., Serrano, R., and Vicente, O.** (2006). Overexpression of *Arabidopsis thaliana* LTL1, a salt-induced gene encoding a GDSL-motif lipase, increases salt tolerance in yeast and transgenic plants. *Plant Cell Environ.* **29**: 1890–1900.
- Nawrath, C.** (2006). Unraveling the complex network of cuticular structure and function. *Curr. Opin. Plant Biol.* **9**: 281–287.
- Oh, I.S., Park, A.R., Bae, M.S., Kwon, S.J., Kim, Y.S., Lee, J.E., Kang, N.Y., Lee, S., Cheong, H., and Park, O.K.** (2005). Secretome analysis reveals an *Arabidopsis* lipase involved in defense against *Alternaria brassicicola*. *Plant Cell* **17**: 2832–2847.
- Osman, S.F., Irwin, P., Fett, W.F., O'Connor, J.V., and Parris, N.** (1999). Preparation, isolation, and characterization of cutin monomers and oligomers from tomato peels. *J. Agric. Food Chem.* **47**: 799–802.
- Panikashvili, D., Savaldi-Goldstein, S., Mandel, T., Yifhar, T., Franke, R.B., Höfer, R., Schreiber, L., Chory, J., and Aharoni, A.** (2007). The *Arabidopsis* *DESPERADO/AtWBC11* transporter is required for cutin and wax secretion. *Plant Physiol.* **145**: 1345–1360.

- Panikashvili, D., Shi, J.X., Schreiber, L., and Aharoni, A.** (2009). The *Arabidopsis* DCR encoding a soluble BAHD acyltransferase is required for cutin polyester formation and seed hydration properties. *Plant Physiol.* **151**: 1773–1789.
- Panikashvili, D., Shi, J.X., Schreiber, L., and Aharoni, A.** (2011). The *Arabidopsis* ABCG13 transporter is required for flower cuticle secretion and patterning of the petal epidermis. *New Phytol.* **190**: 113–124.
- Park, J.J., Jin, P., Yoon, J., Yang, J.I., Jeong, H.J., Ranathunge, K., Schreiber, L., Franke, R., Lee, I.J., and An, G.** (2010). Mutation in Wilted Dwarf and Lethal 1 (WDL1) causes abnormal cuticle formation and rapid water loss in rice. *Plant Mol. Biol.* **74**: 91–103.
- Perrocheau, L., Rogniaux, H., Boivin, P., and Marion, D.** (2005). Probing heat-stable water-soluble proteins from barley to malt and beer. *Proteomics* **5**: 2849–2858.
- Pollard, M., Beisson, F., Li, Y., and Ohlrogge, J.B.** (2008). Building lipid barriers: Biosynthesis of cutin and suberin. *Trends Plant Sci.* **13**: 236–246.
- Pruitt, R.E., Vielle-Calzada, J.P., Ploense, S.E., Grossniklaus, U., and Lolle, S.J.** (2000). FIDDLEHEAD, a gene required to suppress epidermal cell interactions in *Arabidopsis*, encodes a putative lipid biosynthetic enzyme. *Proc. Natl. Acad. Sci. USA* **97**: 1311–1316.
- Queiroz, D.P., de Pinho, M.N., and Dias, C.** (2003). ATR-FTIR studies of poly(propylene oxide)/polybutadiene bi-soft segment urethane/urea membranes. *Macromolecules* **36**: 4195–4200.
- Rani, S.H., Krishna, T.H., Saha, S., Negi, A.S., and Rajasekharan, R.** (2010). Defective in cuticular ridges (DCR) of *Arabidopsis thaliana*, a gene associated with surface cutin formation, encodes a soluble diacylglycerol acyltransferase. *J. Biol. Chem.* **285**: 38337–38347.
- Reina, J.J., Guerrero, C., and Heredia, A.** (2007). Isolation, characterization, and localization of AgaSGNH cDNA: A new SGNH-motif plant hydrolase specific to *Agave americana* L. leaf epidermis. *J. Exp. Bot.* **58**: 2717–2731.
- Reina-Pinto, J.J., and Yephremov, A.** (2009). Surface lipids and plant defenses. *Plant Physiol. Biochem.* **47**: 540–549.
- Rose, J.K., Braam, J., Fry, S.C., and Nishitani, K.** (2002). The XTH family of enzymes involved in xyloglucan endotransglucosylation and endohydrolysis: Current perspectives and a new unifying nomenclature. *Plant Cell Physiol.* **43**: 1421–1435.
- Round, A.N., Yan, B., Dang, S., Estephan, R., Stark, R.E., and Batteas, J.D.** (2000). The influence of water on the nanomechanical behavior of the plant biopolyester cutin as studied by AFM and solid-state NMR. *Biophys. J.* **79**: 2761–2767.
- Sagane, Y., Nakagawa, T., Yamamoto, K., Michikawa, S., Oguri, S., and Momonoki, Y.S.** (2005). Molecular characterization of maize acetylcholinesterase: A novel enzyme family in the plant kingdom. *Plant Physiol.* **138**: 1359–1371.
- Saladié, M., et al.** (2007). A reevaluation of the key factors that influence tomato fruit softening and integrity. *Plant Physiol.* **144**: 1012–1028.
- Schnurr, J., Shockey, J., and Browse, J.** (2004). The acyl-CoA synthetase encoded by LACS2 is essential for normal cuticle development in *Arabidopsis*. *Plant Cell* **16**: 629–642.
- Schönherr, J., and Riederer, M.** (1986). Plant cuticles sorb lipophilic compounds during enzymatic isolation. *Plant Cell Environ.* **9**: 459–466.
- Shi, J.X., Malitsky, S., De Oliveira, S., Branigan, C., Franke, R.B., Schreiber, L., and Aharoni, A.** (2011). SHINE transcription factors act redundantly to pattern the archetypal surface of *Arabidopsis* flower organs. *PLoS Genet.* **7**: e1001388.
- Sieber, P., Schorderet, M., Ryser, U., Buchala, A., Kolattukudy, P., Métraux, J.P., and Nawrath, C.** (2000). Transgenic *Arabidopsis* plants expressing a fungal cutinase show alterations in the structure and properties of the cuticle and postgenital organ fusions. *Plant Cell* **12**: 721–738.
- Takahashi, K., Shimada, T., Kondo, M., Tamai, A., Mori, M., Nishimura, M., and Hara-Nishimura, I.** (2010). Ectopic expression of an esterase, which is a candidate for the unidentified plant cutinase, causes cuticular defects in *Arabidopsis thaliana*. *Plant Cell Physiol.* **51**: 123–131.
- Taketa, S., et al.** (2008). Barley grain with adhering hulls is controlled by an ERF family transcription factor gene regulating a lipid biosynthesis pathway. *Proc. Natl. Acad. Sci. USA* **105**: 4062–4067.
- Tanaka, T., Tanaka, H., Machida, C., Watanabe, M., and Machida, Y.** (2004). A new method for rapid visualization of defects in leaf cuticle reveals five intrinsic patterns of surface defects in *Arabidopsis*. *Plant J.* **37**: 139–146.
- Teutschbein, J., Gross, W., Nimtz, M., Milkowski, C., Hause, B., and Strack, D.** (2010). Identification and localization of a lipase-like acyltransferase in phenylpropanoid metabolism of tomato (*Solanum lycopersicum*). *J. Biol. Chem.* **285**: 38374–38381.
- Updegraff, E.P., Zhao, F., and Preuss, D.** (2009). The extracellular lipase EXL4 is required for efficient hydration of *Arabidopsis* pollen. *Sex. Plant Reprod.* **22**: 197–204.
- Upton, C., and Buckley, J.T.** (1995). A new family of lipolytic enzymes? *Trends Biochem. Sci.* **20**: 178–179.
- Volokita, M., Rosilio-Brami, T., Rivkin, N., and Zik, M.** (2011). Combining comparative sequence and genomic data to ascertain phylogenetic relationships and explore the evolution of the large GDSL-lipase family in land plants. *Mol. Biol. Evol.* **28**: 551–565.
- Waltson, T.** (1990). Waxes, cutin and suberin. In *Lipids, Membranes and Aspects of Photobiology*, E.J. Harwood and J. Boyer, eds (London: Academic Press), pp. 105–158.
- Wellesen, K., Durst, F., Pinot, F., Benveniste, I., Nettesheim, K., Wisman, E., Steiner-Lange, S., Saedler, H., and Yephremov, A.** (2001). Functional analysis of the LACERATA gene of *Arabidopsis* provides evidence for different roles of fatty acid omega-hydroxylation in development. *Proc. Natl. Acad. Sci. USA* **98**: 9694–9699.
- Xiao, F., Goodwin, S.M., Xiao, Y., Sun, Z., Baker, D., Tang, X., Jenks, M.A., and Zhou, J.M.** (2004). *Arabidopsis* CYP86A2 represses *Pseudomonas syringae* type III genes and is required for cuticle development. *EMBO J.* **23**: 2903–2913.
- Yang, W., Pollard, M., Li-Beisson, Y., Beisson, F., Feig, M., and Ohlrogge, J.** (2010). A distinct type of glycerol-3-phosphate acyltransferase with sn-2 preference and phosphatase activity producing 2-monoacylglycerol. *Proc. Natl. Acad. Sci. USA* **107**: 12040–12045.
- Yeats, T.H., Howe, K.J., Matas, A.J., Buda, G.J., Thannhauser, T.W., and Rose, J.K.** (2010). Mining the surface proteome of tomato (*Solanum lycopersicum*) fruit for proteins associated with cuticle biogenesis. *J. Exp. Bot.* **61**: 3759–3771.
- Yeats, T.H., Martin, L.B., Viart, H.M., Isaacson, T., He, Y., Zhao, L., Matas, A.J., Buda, G.J., Domozych, D.S., Clausen, M.H., and Rose, J.K.** (May 20, 2012). The identification of cutin synthase: Formation of the plant polyester cutin. *Nat. Chem. Biol.* <http://dx.doi.org/10.1038/nchembio.960>.
- Zhou, S., Sauvé, R., and Thannhauser, T.W.** (2009). Proteome changes induced by aluminium stress in tomato roots. *J. Exp. Bot.* **60**: 1849–1857.
- Zlotnik-Mazori, T., and Stark, R.E.** (1988). Nuclear magnetic resonance studies of cutin, an insoluble plant polyester. *Macromolecules* **21**: 2412–2417.



**Supplemental figure 1:** Expression pattern of *SIGDSL1* in Ailsa Craig fruit tissues. Transcript abundance was measured by real time RT-PCR in exocarp, mesocarp, locular tissue, columella and seeds of fruits at 12, 20, 27 and 35 DPA. *EiF4 $\alpha$* ,  $\beta$ -tubulin and actin were used as housekeeping genes to calculate transcript relative expression AU = arbitrary units. Vertical bars represent standard deviation (n=4).

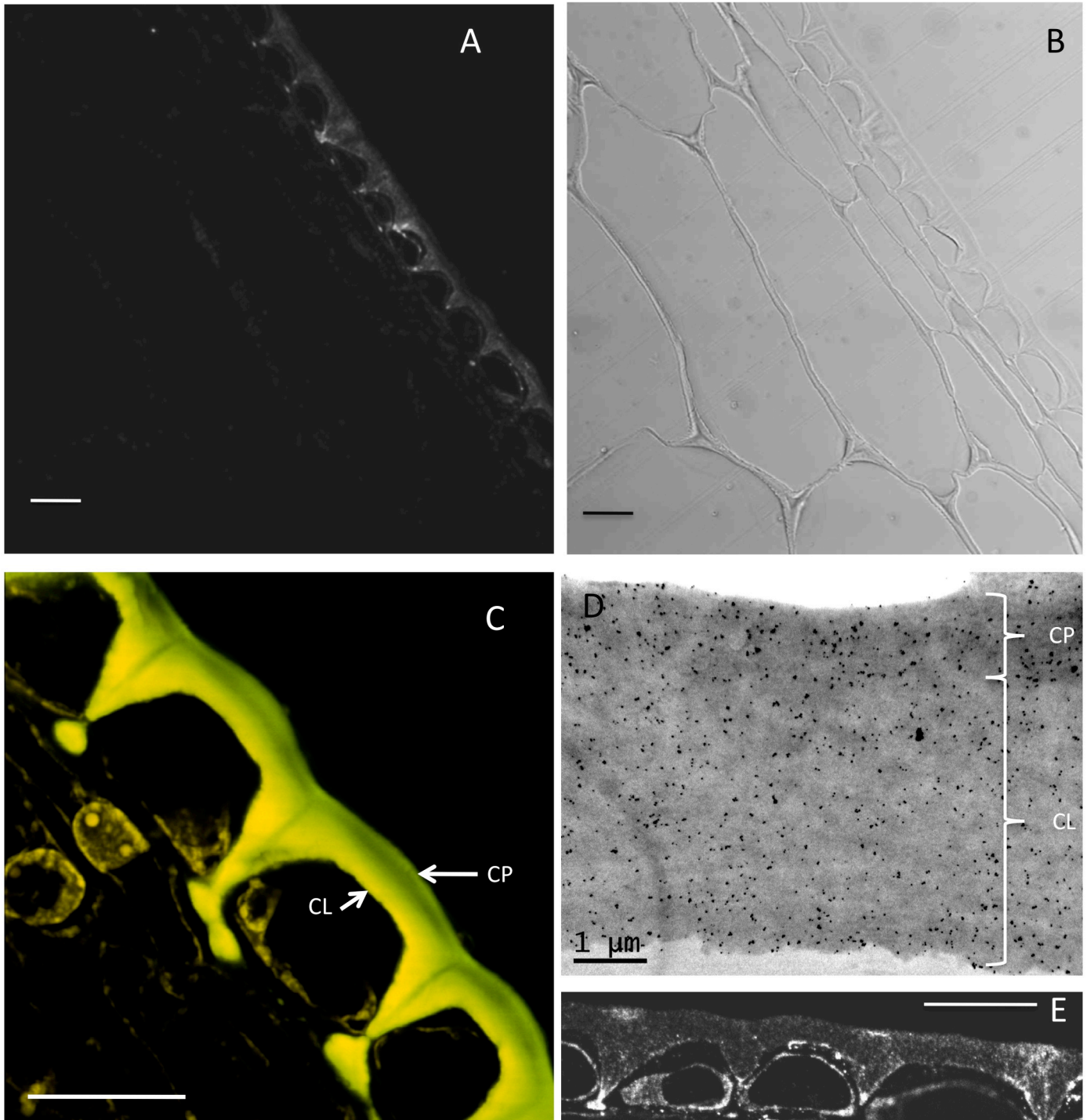
```

acaaccaatttataatatttttgaacaacacttttttttttttttttttggccaaatggcc
acacctactattattttgagcttcttggttgattttttggagtggttattttgtcaaagtMAgaa
T P T I I L S F L L I F G V A I C Q S E
gctagggcatatttttgggtgattcacttggatagtggaataataattattttg
A R A F F V F G D S* L V D S G N N N Y L
gctactactgcaagggctgattcaccaccttatgggtattgattatccaacacgtagagca
A T T A R A D S P P Y G I D Y P T R R A
actggtcgtttctctaatggctacaacattcctgacattatcagtcaacaaattggttca
T G R F S N G Y N I P D I I S Q Q I G S
tcagagtcaccactaccttacttagatccagctcttactggacaaagacttcttggttgg
S E S P L P Y L D P A L T G Q R L L V G
gctaactttgcatctgctggaattggaataactaaatgacactggaatccaatttattaat
A N F A S A G I G I L N D T G I Q F I N
attattcgaatgccacaacaattggcttatttttagacaatatcaaagtagagtaagtggc
I I R M P Q Q L A Y F R Q Y Q S R V S G
cttattgggtgaagcaaataactcaaagacttgtaaatacaagctcttggttcttatgactctt
L I G E A N T Q R L V N Q A L V L M T L
ggaggcaatgattttgtcaacaactattatcttgtgcccaattctgcgcgatcacgcaa
G G N D* F V N N Y Y L V P N S A R S R Q
ttttctattcaagattatgtcccttattttgataagagaatatcgtaaaatcttgatgaat
F S I Q D Y V P Y L I R E Y R K I L M N
gtgtataatcttggagctcgtcgtgtaattgtaactggaactggaccggttagggtgtgtt
V Y N L G A R R V I V T G T G P L G C V
ccagcagaactagctcaacgtagcaggaacggggaatgttcacccgagttgcaacgagct
P A E L A Q R S R N G E C S P E L Q R A
gcaggcctgtttaacccccagcttacgcaaagtgtgcaggggttaaatagtgaactaggc
A G L F N P Q L T Q M L Q G L N S E L G
agcgatgtttttattgctgcaatacacacaacaatgcatacgaatttcattactaatcca
S D V F I A A N T Q Q M H T N F I T N P
caagcatatggatttataacatcaaaggtagcatgttgggacaaggaccatataacggt
Q A Y G F I T S K V A C C G Q G P Y N G
cttggctatgtacaccgctctctaattttgtgcccgaaatagagatgtttacgcgttttgg
L G L C T P L S N L C P N R D V Y A F W
gaccggttccatccatctgagagggcaataagatcattgtgcagcaaatcatgtctggt
D* P F H* P S E R A N K I I V Q Q I M S G
acaacggagcttatgaatccaatgaatctcagtacgattctggctatggattcacatgca
T T E L M N P M N L S T I L A M D S H A
taagacatatctaagatatctggaatctgattcacttgtacttttttgttgctaatttt
tggtataaataagatgtatgcaacacttcatgttggctacttttaatttacaacaaaa

```

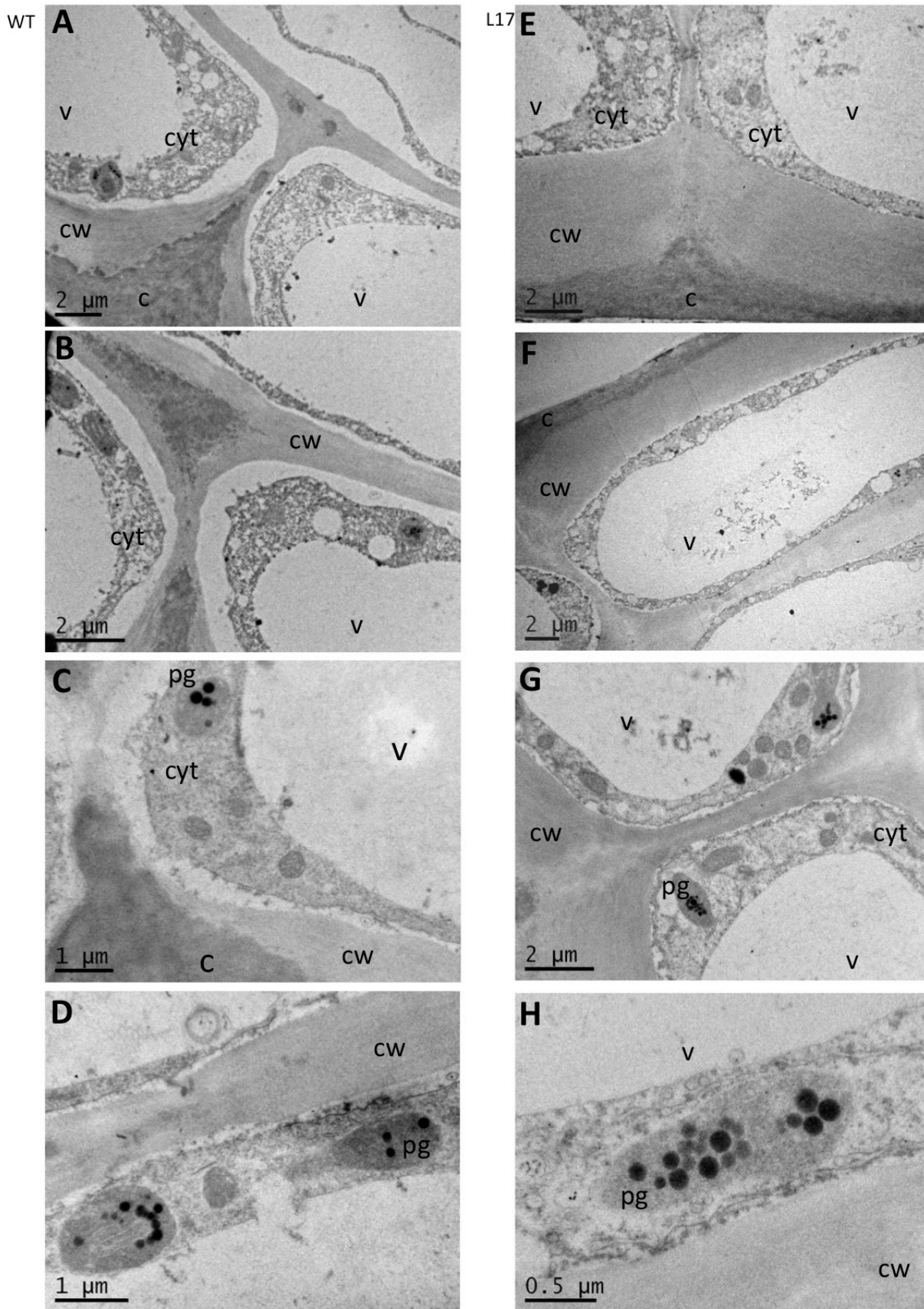
**Supplemental figure 2.** Nucleotide and deduced protein sequences of *GDSL1*.

Start and stop codons are indicated in bold. The N-terminus signal peptide is marked in blue. G-D-S-L tetrapeptide motif (in red) is located close to the N-terminal region. The conserved regions of protein sequence are indicated by black boxes and green letters. Block I, III and V contain the classical catalytic triad (\*): serine, acid aspartic and histidine.

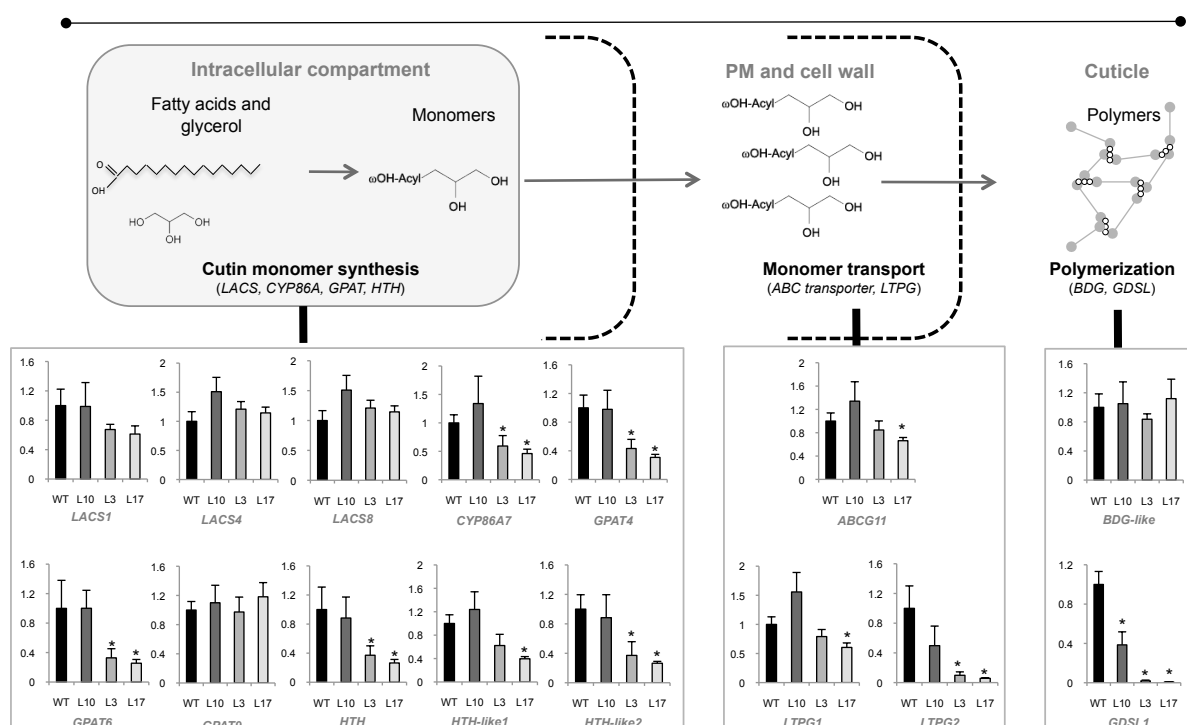


**Supplemental figure 3.** Localization of SIGDSL1 in 20 DPA tomato fruit cuticle.

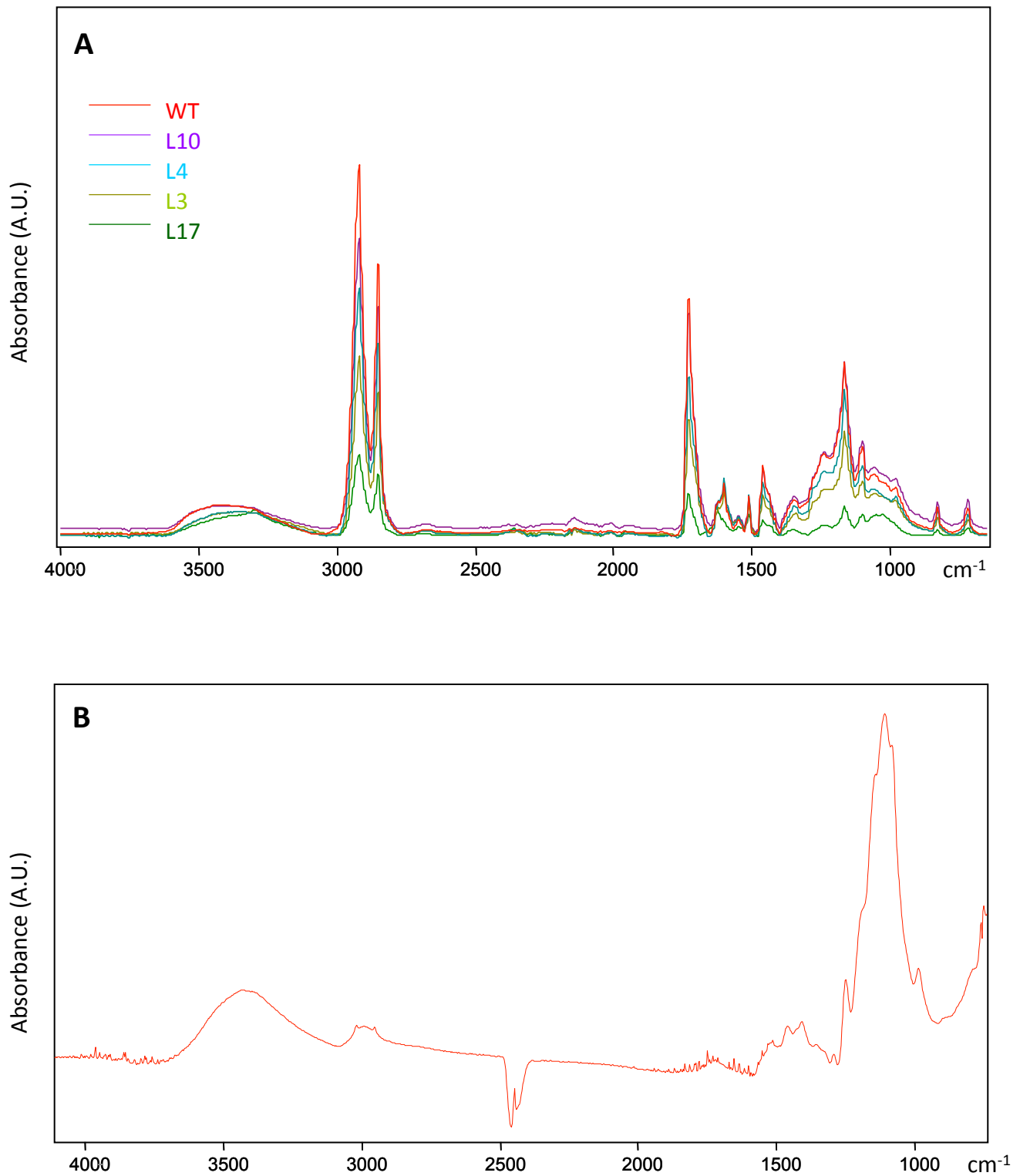
(A) Immunofluorescence detection of SIGDSL1 and (B) bright field micrograph of WT tomato exocarp, showing that SIGDSL1 labeling is restricted to the cuticle and to the cytoplasm of epidermal cells. (C) Auramine O staining of fruit cuticle. CP, cuticle proper; CL, cuticle layer. (D and E) TEM and fluorescence microscopy showing SIGDSL1 immunolabeling in both CP and CL. Bars= 20mm.



**Supplemental figure 4.** Ultrastructural feature of epidermal cells of cutinized exocarps. Osmium labelled lipids in 20 DPA tomato exocarp of WT (A-E), and transgenic line L-17 (F-H).v: vacuole, cl: cuticle; cw: cell wall; cyt: cytoplasm; pg:plastoglobule



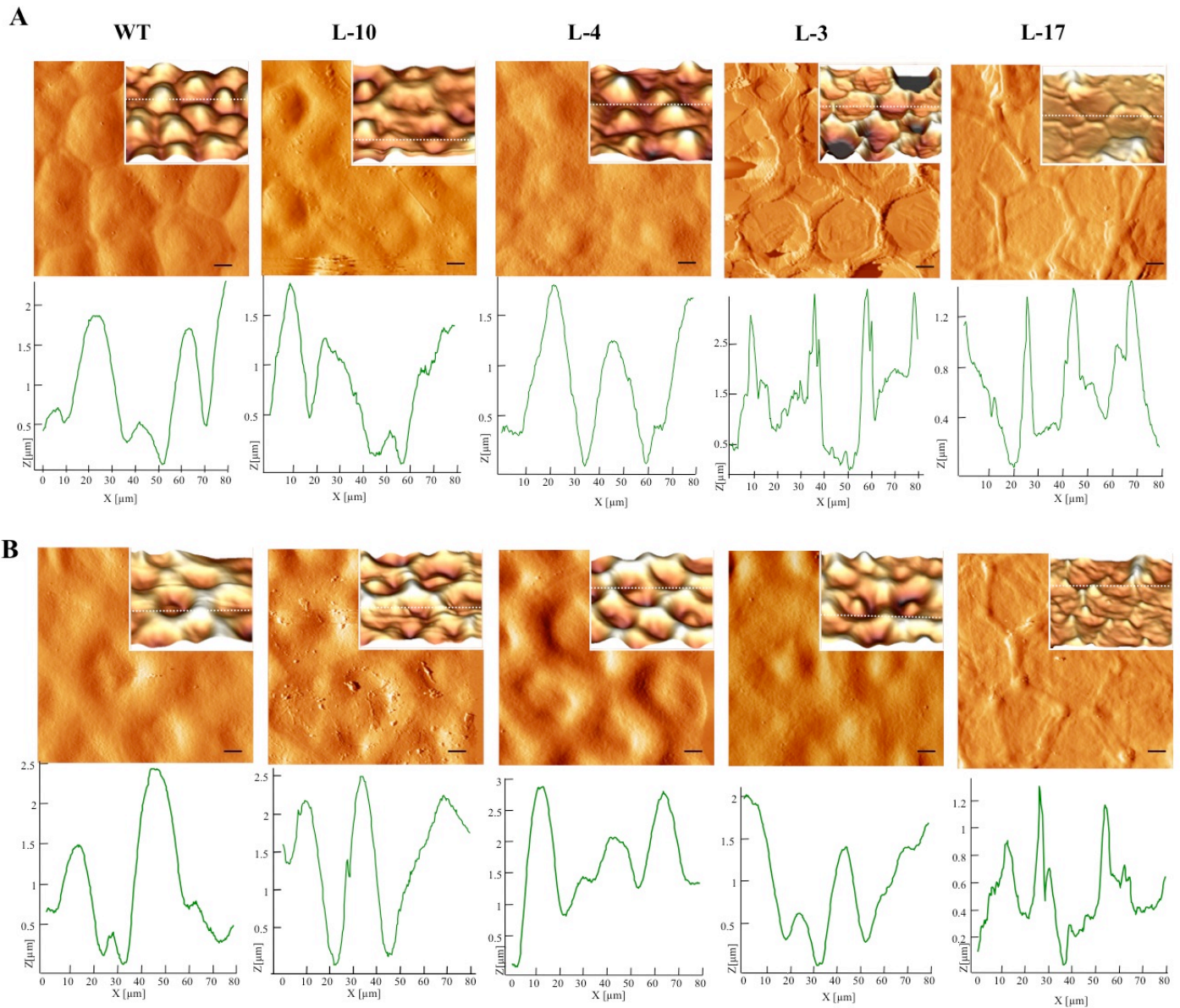
**Supplemental figure 5.** Transcript levels of cutin-associated genes in WT and P35S-SIGDSL1 RNAi transgenic lines. Transcript abundance was measured by real time RT-PCR in 20 DPA fruit exocarp from WT and L-10, L-3 and L-17 lines. Eif4 $\alpha$ ,  $\beta$ -tubulin were used as housekeeping genes to calculate transcript relative expression. Gene information is given in Supplemental Table 1. Values represent means and standard errors (n = 4) in arbitrary units and \* indicates significant differences compared to WT control (P<0.05) obtained with a Student's t test.



**Supplemental figure 6.** Total ATR FT-IR spectra .

(A) isolated cutin absorbance. Analyses were performed on isolated cutin of Breaker + 7 days fruits from WT and P<sub>35S</sub>*SIGDSL1*<sup>RNAi</sup> plants.

(B) Residue after alkaline hydrolysis of WT cutin



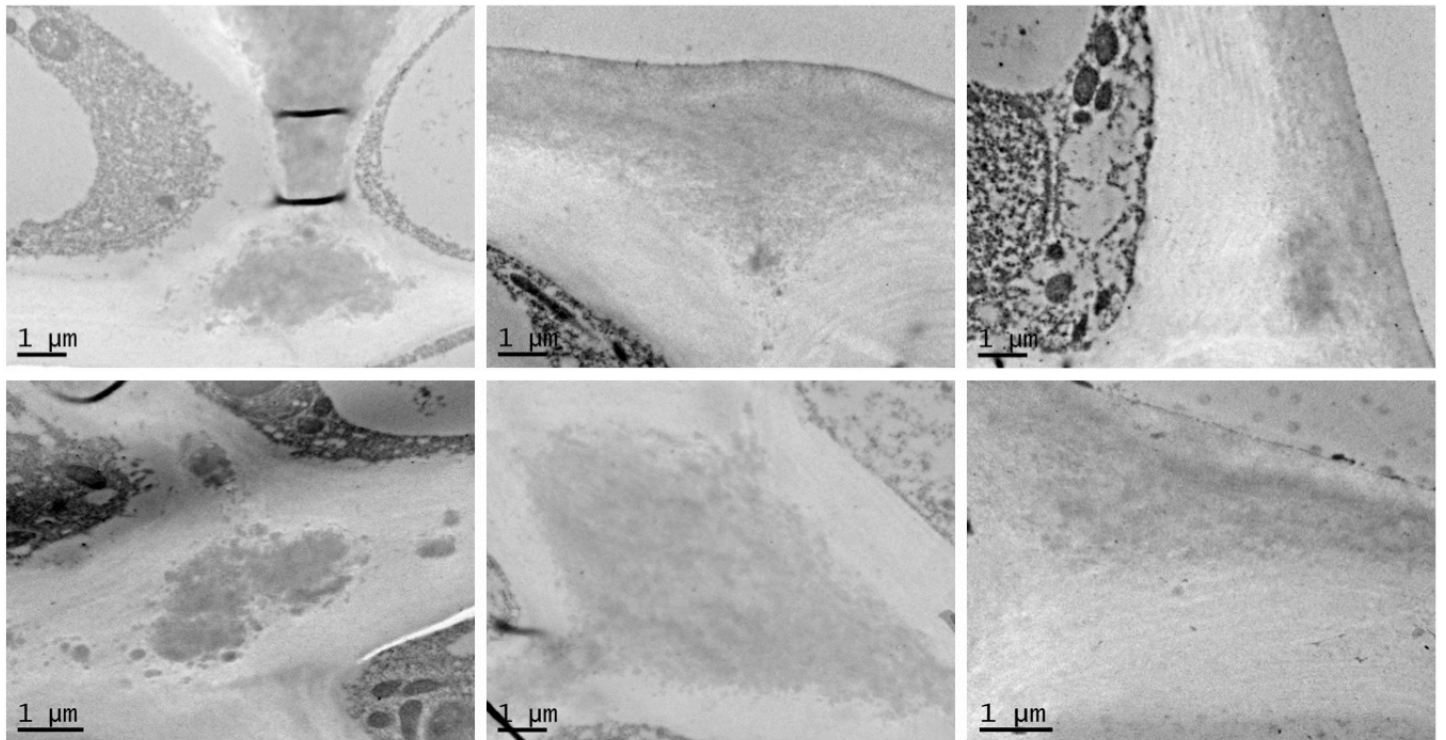
**Supplemental figure 7.** AFM images of tomato cutin surfaces of fruits from WT and *P35S-SIGDSL1* RNAi plants at 20 DPA and breaker + 7 days stages.

Error signal images were recorded in tapping mode at 80 $\mu$ m X80  $\mu$ m magnification at 20 DPA (A) and breaker + 7 days (B) stages. For each sample, the corresponding 3D height image is presented in inset. The linear profile is drawn from the height image (dotted line in inset). Bars represent 8  $\mu$ m.

WT

L3

L17



**Supplemental figure 8:** Immunolabeling of tomato exocarp with pre-immune sera  
The exocarp of WT and P35S-SIGDSL1 RNAi L-3 and L-17 lines 20 DPA fruits were treated with pre-immune serum at the same concentration as the polyclonal antibody (Figure 6).

Supplemental Data. Girard et al. (2012). Plant Cell 10.1105/tpc.112.101055

Real time PCR analyses: primer sequence

Gene name	SGN Accession Number	Blast P TAIR Arabidopsis		E-value	5' primer	3' primer	Amplification size	mean CT (WT)
		Gene accession number	Identification					
<b>Cutin monomer synthesis</b>								
<i>SILACS1</i>	SGN-U573278	AT2G47240	LACS1	0.0	CAATCCACTGCATGATCGTC	CGCTAGAAGGGTGCTTAAATTAGA	141	24.55
<i>SILACS4</i>	SGN-U575624	AT4G23850	LACS4	e-171	CCCAGATGCTCAAATTTTACAAG	CACCTTGACTACAGTCAAACCCAGTT	218	28.57
<i>SILACS8</i>	SGN-U569341	AT2G04350	LACS8	0.0	TTTTGCTGTTGCGTCAATGT	GCGAGGCGAGAACAAAATCT	98	25.12
<i>SIGPAT4</i>	SGN-U578399	AT1G01610	GPAT4	0.0	GGTGAAATGATGGCAAAGT	CAGAATCCCTCTCAAAGCA	101	19.56
<i>SIGPAT6</i>	SGN-U573482	AT2G38110	GPAT6	0.0	GTCGCGTTGCAATAAAGGAC	TGTTTTCTTTTCAATTCTCTTGA	142	22.6
<i>SIGPAT9</i>	SGN-U577121	AT5G60620	GPAT9	0.0	TCTCCATGTTCCACTCTTGC	GGCTTCACAGACATTGTTGC	135	25.22
<i>SICYP86A7</i>	SGN-U563152	AT1G63710	CYP86A7	e-161	TGCAGTAAATGGAATTGCAGCT	CATTATTTGCTTATAGCCACATTCA	146	22.82
<i>SIHTH</i>	SGN-U575460	AT1G72970	Hothead, HTH	0.0	AGCAAGCAAGTGTGTAGTCTGT	GCACAAAAGTCCAATTCCA	96	20.67
<i>SIHTH like1</i>	SGN-U570812	AT1G12570	HTH-like	0.0	AGCCACTGTATGATGCTTG	TCCACTCTCATTCAAACAAAAGA	137	21.62
<i>SIHTH like2</i>	SGN-U570813	AT5G51950	HTH-like	e-174	TCGCATTTAATTTGGGAAT	AACAATAATGACCCTTCCGTTTT	117	19.43
<b>Monomer transport</b>								
<i>SIABCG11</i>	SGN-U572046	AT1G17840	ABCG11	e-151	CTCAGGGCCTATGTTGGAAA	GCCTCCATGCATATTTCTTCTT	113	25.12
<i>SILTPG1</i>	SGN-U581465	AT2G38540	LTP1	1.00E-20	CAGCCCCCTACTGACTGCT	TCAAATTCGAAAACAGACTCG	199	19.44
<i>SILTPG2</i>	SGN-U579033	AT2G38540	LTP1	4.00E-11	TGGCTTGAGAGATGAAGAA	CCAATGTTCAACAAGACTCGAC	148	18.54
<b>Polymerisation</b>								
<i>SIBdg-like</i>	SGN-U570965	AT1G64670	Bodyguard	3.00E-68	AGAGAAGCTATGGGATCAATATGT	GCTTTCACCAATGTCATTACAAA	105	31.35
<i>SIGDSL1</i>	SGN-U585129	AT5G33370	GDSL-like Lipase/Acylhydrolase	e-153	CAATATCACACTCCACCCACAAA	GCAACACTTCATGTTGTGCTACTT	110	18.15
<b>Reference genes</b>								
<i>EIF4a</i>	SGN-U578071				AGTGGACGATTTGGAAGGAAG	GCTCCTCGATTACGACGTTG	106	19.73
<i>b-tubulin</i>	SGN-U564000				AACCTCTCGTGGATCACAGC	GGCAGAAGCTGTCAGGTAACG	127	20.09
<i>Actin</i>	SGN-U579547				GGACTCTGGTATGGTGTAG	CCGTTACAGCAGTAGTGTTG	160	19.12

**Supplemental table I: Accession and sequence information concerning real-time RT PCR primers**

Accession numbers are indexed in SOL Genomics Network database (<http://www.sgn.cornell.edu/>) and TAIR Arabidopsis Information Resource database (<http://www.arabidopsis.org/>). Tomato homologs of *Arabidopsis thaliana* genes involved in the regulation (*SHN*), synthesis (*LACS*, *CYP86A*, *GPAT*, *HTH*), transport (*ABCG*) and polymerization (*BDG*) of cutin were identified by Blast search (protein sequences) of the SGN tomato unigene database (<http://solgenomics.net/>), which represents all the tomato-expressed genes. Tomato genes were further selected according to their Blast score (E-value) and named according to their closest homolog in *Arabidopsis*. The *SILTPG1* and *SILTPG2* genes were already described in tomato (Le et al., 2006). Their *Arabidopsis* putative orthologs were identified by BlastP search of the TAIR database (<http://www.arabidopsis.org/>), as for *SIGDSL1*. The two last columns presents the length of amplification products (units = pb, pair of bases) and the mean CT obtained for WT in real time PCR. Primer lengths were restricted to 20 to 26 pb in the 3' UTR. Careful attention was given to avoid secondary structures forming regions using mfold software (<http://www.bioinfo.rpi.edu/applications/mfold/cgi-bin/dna-form1.cgi>).